Summer 2017

Geomechanical analysis of the wellbore instability problems in Nahr Umr Formation southern Iraq

Haider Qasim Mohammed

Department:

GEOMECHANICAL ANALYSIS OF THE WELLBORE INSTABILITY PROBLEMS IN NAHR UMR FORMATION SOUTHERN IRAQ

by

HAIDER QASIM MOHAMMED

A THESIS

Presented to the Faculty of the Graduate School of the

MISSOURI UNIVERSITY OF SCIENCE AND TECHNOLOGY

In Partial Fulfillment of the Requirements for the Degree

MASTER OF SCIENCE IN PETROLEUM ENGINEERING

2017

Approved by

Ralph E. Flori , Advisor
Shari Dunn-Norman
Peyman Heidari

ABSTRACT

Wellbore instability problems play a major rule of increasing nonproductive time (NPT) during drilling processes. In most cases, the cost of drilling a well can be reduced by designing a suitable operational window using geomechanical models. Several wellbore instability problems have been encountered during drilling Nahr Umr Formation in an oil field in southern Iraq. These problems include but are not limited to, mechanical stuck, caving, and tight holes. Data from twenty vertical wells are investigated to reveal the major factors that control the instability problems and to design an optimum mud window. A geomechanical model is developed to determine the in-situ stress and induced stresses by using numerous field and laboratory data for Nahr Umr Formation. Mohr-Coulomb and Mogi-Coulomb failure criteria are used to predict the breakout profile and to estimate the optimum mud weight to avoid sticking. Our analysis shows that the majority of wellbore instability problems are mainly caused by, rock failure (shear failure) around the wellbore due to high stresses and low rock strength, and inappropriate drilling practice with respect to the heterogeneity of Nahr Umr Formation. Moreover, the wellbore failure analysis demonstrates the necessity of core analyses and field tests such as the triaxial test and the mini-frac. test to improve the geomechanical model when studying lithology with high heterogeneity.

ACKNOWLEDGMENT

I would like to express my sincere appreciation to my supervisor, Dr. Flori, for his constant guidance and encouragement throughout this thesis.

I would like to thank my committee, Dr. Shari Dunn-Norman and Dr. Peyman Heidari, for their assistance and suggestion.

I would like to express my heartfelt gratitude to the Zubair field operation division (ZFOD) of south oil company for granting my data for this study.

My deepest gratitude goes to the Higher Committee for Education Development in Iraq (HCED) for awarding me a fully funded scholarship.

I am extremely grateful to my friends and colleagues at the Missouri university of Science and Technology for their moral support and for being a source of motivation.

Words can never be enough to express my gratitude to my family. Special thanks to my parents and siblings for their love, encouragement, and support throughout the period of my studies. Without them, I may never have reached the level where I am today.

TABLE OF CONTENTS

LIST OF ILLUSTRATIONS

Page

LIST OF TABLES

Page

NOMENCLATURE

Symbol	Description
σ	Stress
ε	Strain
τ	Shear stress
E	young's modulus
F	Force
A	Area
ν	Poisson's ratio
V_p	Compressional Velocity
V_s	Shear Velocity
S_v	Vertical stress
S_H	Maximum horizontal stress
S_h	Minimum horizontal stress
ρ_a	Average density
ρ_b	Bulk density
Z	Depth
ρ_m	Matrix density
ρ_f	Fluid density
P_p	Pore pressure
ϕ	Fprmation porosity
α	Biot's Coefficient

R	Shale resistivity
R_n	Shale resistivity at normal hydrostatic pressure
σ_r	Radial stress
σ_z	Axial stress
σ_θ	Hoop stress
P_w	Drilling mud pressure
a	Wellbore radius
S_o	Cohesion
φ	Friction angle
V_{shale}	Shale Volume
GR	Gamma ray
Δt	Compressional Travel Time
μ	Coefficient of the Internal Friction angle
T_o	Tensile strength
NPT	Non- productive time
BHA	Bottom hole assembly
RFT	Repeat formation test
Mw	Mud weight
NF	Normal fault
SS	Strike-Slip fault
RF	Reverse fault
USBM	United states Bureau of mines

CSIRO	Common wealth scientific and industrial research organization
LOT	Leak-off test
XLOT	Extended leak-off test
FIP	Fracture Propagation pressure
LOP	Leak-off point
FPP	Fracture propagation pressure
ISIP	Instantaneous shut-in pressure
FPP	Fracture closure pressure
UCS	Unconfined compressive strength
ASTM	American society for testing and material

1. INTRODUCTION

H field is one of the mature oil fields in southern Iraq. It was discovered in 1949 and went on stream in 1951. The field structure includes four reservoirs: upper sand member, Mishrif carbonate, upper and lower sandstone (3rd pay and 4th pay). The structural trap of H field is a large gentle anticline oriented north/northwest to south/southeast approximately 60 km long and 10-15 km wide. H Field consist of four domes divided by saddles; from the northwest to southeast are dome 1, dome 2, dome 3, and dome 4. From a genetic point of view, the tectonic deformation of the structure of H field are related to the following two reasons: uplift of basement rocks and salt tectonics. Dome 1 culmination was formed mainly by salt tectonics, whereas dome 2 culmination was formed by uplift of basement rocks.

Despite the modern advancement and the usage of new technology in the oil and gas industry, wellbore instability remains one of the most challenging aspects in terms of the cost to drill and complete a well. Eight billion dollars are spent each year due to wellbore instability problems (Peng, 2007), causing an increase in the drilling budget by 10% (Aadnoy, 2003). Therefore, wellbore stability is considered to be one of the major stages of well planning and has been studied extensively (Bell, 2003; Bradley, 1979; Ding, 2011; Zhang et al., 2003; Zhang et al., 2009; Gentzis et al., 2009).

Wellbore instability is dominated by pore pressure, in-situ stresses, and rock strength properties. Prior to drilling a well, the formation is in equilibrium. As soon as the drilling starts, the stresses surrounding the wellbore have to take the load that was taken by the removed rock. Therefore, the in-situ stresses near the borehole wall will be modified, and a stress concentration is present. As a result, the stress concentration will cause a failure

in the borehole wall. The basic problem is to be able to identify the reaction of the rock in respect to the mechanical loading.

However, to avoid the borehole failure, an appropriate internal wellbore pressure (mud pressure) should be altered to adjust the stress concentration. Moreover, borehole orientation with respect to the in-situ stresses should be taken into account to avoid the wellbore failure. The drilling mud pressure is the controllable parameter in any drilling operation, and it can prevent failure if the pressure is still within the bounds of collapse and fracture gradients, in addition to its advantage in eliminating/mitigating the effect of the mechanical wellbore failure **(Bourgoyne et al., 1986).** Drilling mud provides several functions, including cooling and lubricating the drilling bit and drill string, transporting cutting to the surface, transmitting hydraulic energy to the tools and bit through drilling string, and controlling formation pressure. Traditionally, the drilling mud pressure is designed to restrain the flow of the formation fluid into the well regardless of the field stresses and the rock strength effects. Practically, there is a constant pressure, typically 100-200 psi or 0.3 to 0.5 lb/gal mud density greater than the formation pore pressure (French & McLean, 1992; Awal et al., 2001), between the formation pressure and pore pressure to inhibit the flow of the fluid. In general, due to the in-situ stresses, the mud pressure required to sustain the wellbore should be greater than the pressure required to balance. Hence, better approaches should be used to obtain optimum mud pressure based on the accurate estimation of rock properties, stresses around the wellbore, and wellbore trajectory to drill a well safely.

Literature groups wellbore instability failure into mechanical (for instance, high stresses, low rock strength, and inappropriate drilling practice) and chemical (due to the

interaction between drilling fluid and the rock). In many cases, instability may be occur due to a combination of the two failures. Mechanical failures are classified into three categories, as shown in Figure 1.1.

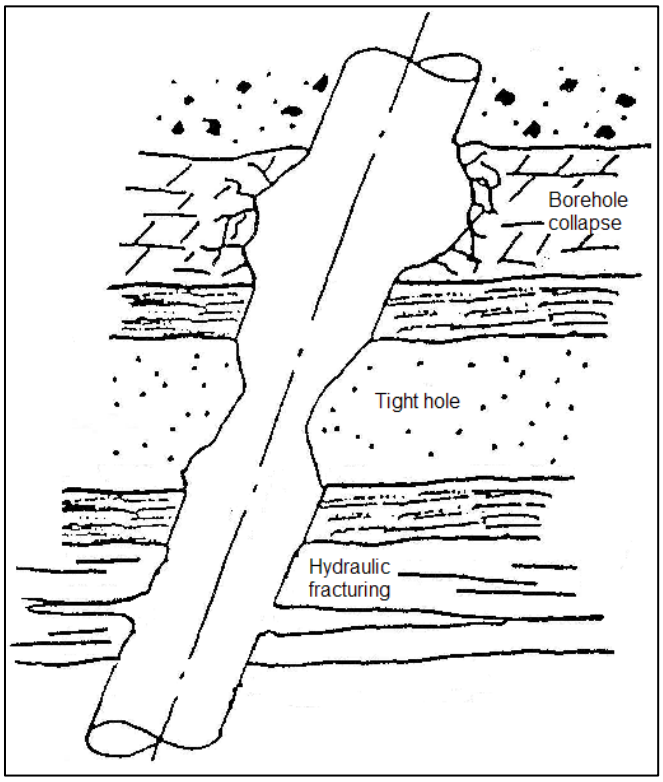

Figure 1.1. Mechanical wellbore failure.

Hole enlargement, or borehole collapse, happens when the mud weight pressure is lower than expected. In other words, the collapse occurs when the stress imposed by drilling mud is less than rock the compressive strength. This type of failure called shear failure. The symptoms of shear failure are poor cementing, increase in hydraulic requirements for effective hole cleaning, and difficulties in run and response of well logging tools. Poor cementing can cause sand control problems and influx of the formation fluid. Moreover, when the hole starts to collapse, the collapsed rock pieces fall down into

the borehole and start to settle on the drill string. This settling prevents the ability to pull out the drill string and leads to stuck pipe. As a result, the drilling operations will halt.

In addition, borehole breakout is known as an enlargement or elongation in the wellbore within a particular direction. This enlargement is considered an important indicator to predict the orientation of minimum horizontal stress. Practically, the borehole enlargement can be predicted by using a 4-6 arm caliper tool, optical imaging log, resistive image log, and acoustic image log (Jaeger et al., 2009; Bell & Gough, 1979; Zoback et al., 1985). Figure 1.2 shows wellbore enlargement pattern via four arm caliper. The four arms caliper has four pads in two calipers: pad 1 and 3 are represented by caliper 1 (C1), while pad 2 and 4 are represented by caliper 2 (C2). The diameter of the hole can be identified from those two calipers. Figure 1.2a shows an in-gauge hole because of the C1 and C2 have the same reading as bit size. In contrast, Figure 1.2c demonstrates a severe washout in the borehole size. This washout is identified through the disparity in C1 and C2 reading.

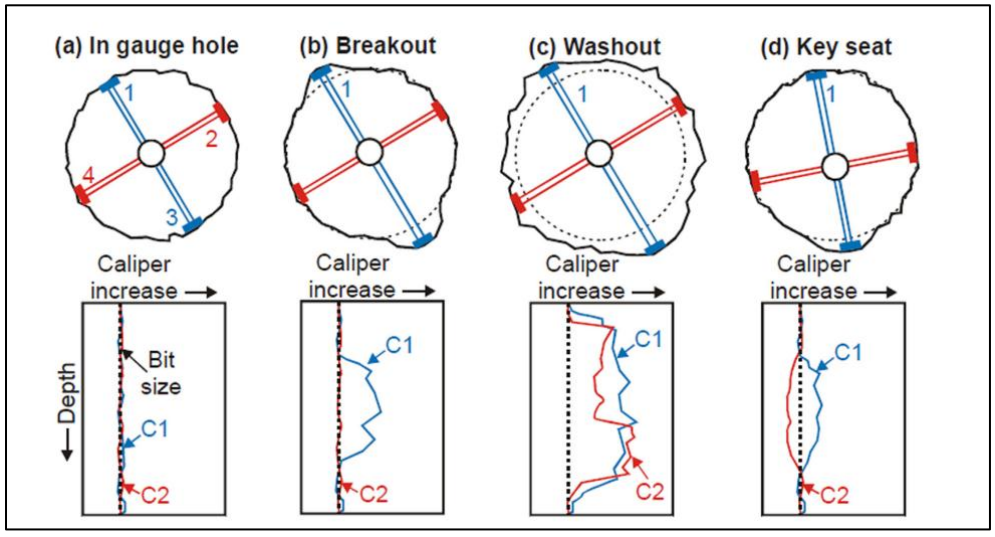

Figure 1.2. Caliper log responses due to wellbore enlargement (Reinecker et al., 2003)

Tight hole or hole sized reduction is a narrowing process of borehole instability. It generally occurs by plastic flow of the rock (creep under the overburden effect) and is usually encountered in shale, sandstone, and salt sections. The consequences of this reduction are increased drag and torque, possible of pipe sticking, and difficult casing landing. Repeat reaming operations are required to prevent these consequences.

Fracturing occurs when the mud weight pressure exceeds the formation fracture pressure. The symptoms of hydraulic fracture are lost circulation and well control problems (kick and blowout). Lost circulation is illustrated as the invasion of drilling fluid into the formation. This invasion will diminish the effect of the applied mud pressure and may result in an inflow of formation fluid. Therefore the pore pressure will flow from a high-pressure zone to a low-pressure zone (loss zone) and cause underground blowout, or kick.

In order to determine wellbore stresses, the rock strength must be known, an appropriate model must be selected, and an accurate rock failure criterion must be chosen. The rock strength is an essential parameter in wellbore stability because it shows the behavior of the rock when it is under the in-situ stress effects. The rock strength properties can be obtained from well logs data and empirical equations (Rahimi, 2014).

Numerous models have been built to identify the induced stress in a circular well and to predict the suitable mud pressure by using failure criteria. Several failure criteria are presented with various characteristics, including 2D or 3D criteria. Among the proposed models, the linear elastic model is likely the most common approach (in synchronism with a linear failure criterion). Frequently, the Mohr-Coulomb failure criterion is the simplest and the most practically used in prediction of borehole breakout. This failure criterion was built based on the assumption that, at the failure, there is a linear increase between the

major, σ_1, and minor, σ_2, principle stresses. Additionally, Mohr assumes that the intermediate principle stress has no effect on rock strength. The Mohr-coulomb criterion was found by several researchers as a deficient and conservative estimation of optimum mud pressure because the intermediate principle stress may feed rock with additional strength. Vernik and Zoback (1992) alluded that the Mohr- Coulomb criterion did not provide realistic results when they made their analysis on crystalline rocks. So, they recommended using a 3D failure criterion (criterion that accounts the intermediate principle stress). In order to meet the needs, Mogi (1971) conducted experimental analyses by using triaxial tests carried out on different types of rock. His analysis unveiled the influence of σ_2 on the rock strength.

In this analysis, two failure criteria have been used to predict the proper mud weight in the Nahr Umr Formation in southern Iraq. The two failure criteria are Mohr-Coulomb and Mogi-Coulomb.

1.1. AN OVERVIEW OF DRILLING CHALLENGES

It reported that approximately 75% of the drilled formations worldwide are shale formations, where 90% of related drilling problems occur (Steiger, 1992). Drilling through a 12.25-in. hole section was investigated for twenty vertical wells in a southern Iraqi oil field. This investigation reveals that several wellbore instability problems have been encountered while drilling that section, such us stuck pipe, partial and total losses, sidetrack, hole pack off, and caving Figure 1.3**.** Some of these problems contributed to the NPT by increasing the time of circulation and reaming. The severity of these problems has caused, in some cases, several sidetracks in one well and/or losing the well. Moreover, the

analysis shows that the majority of instability problems have taken place in Nahr Umr shale formation Figure 1.4**.** A compressive wellbore failure (breakout failure) has been noticed as well. This compressive failure considers as the main causes of hole enlargement, stuck pipe, poor primary cement jobs, and poor log quality while drilling Nahr Umr Formation.

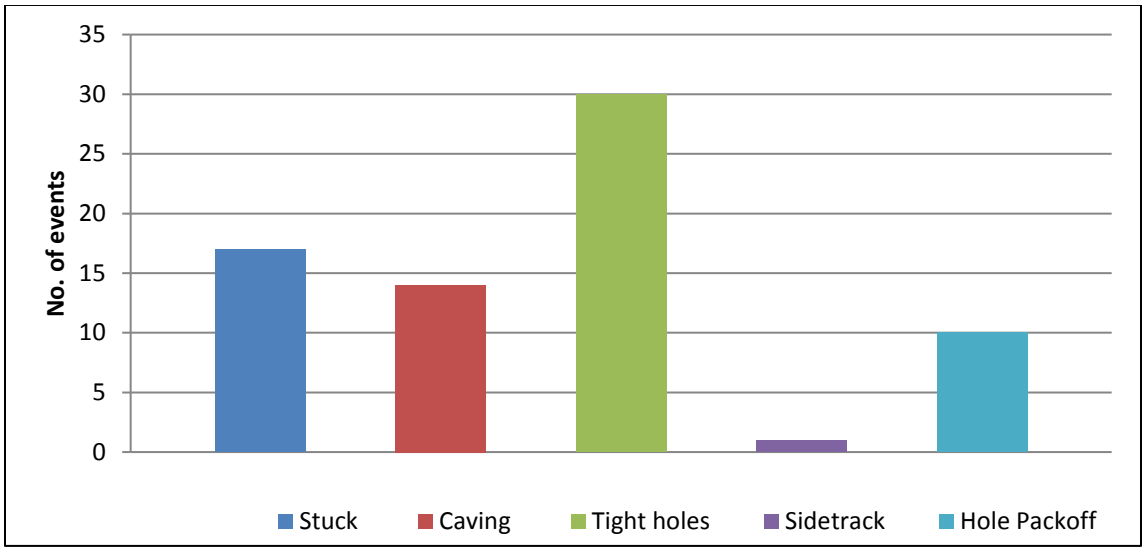

Figure 1.3.Wellbore instability problems in 12.25-in. hole section.

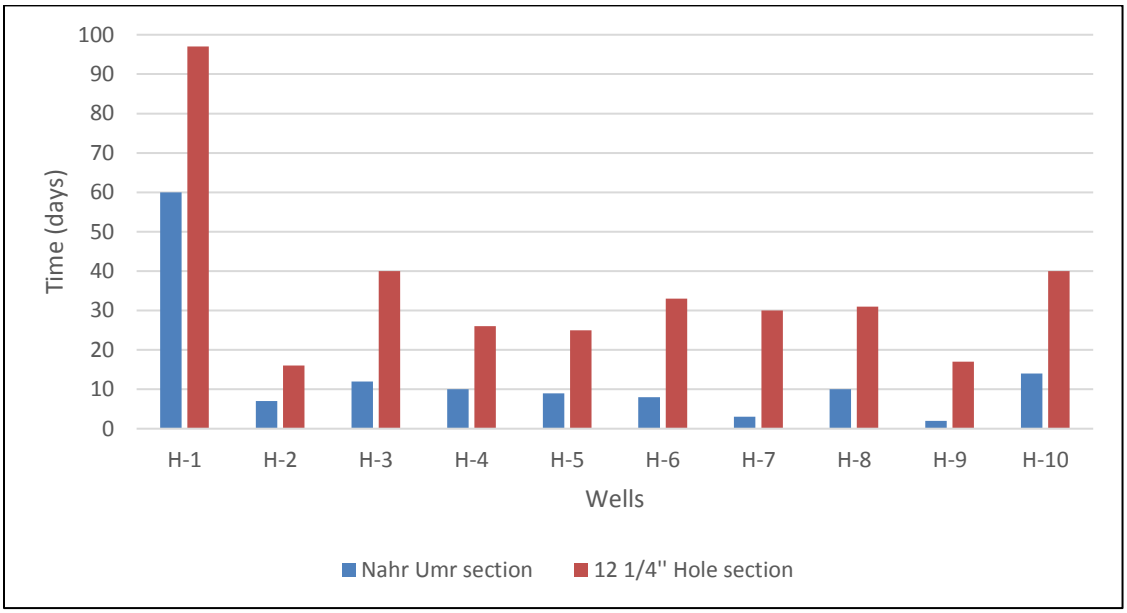

Figure 1.4. The NPT during drilling 12.25-in. hole section and the Nahr Umr Formation.

Stuck pipe incidents are a major drilling problem in the petroleum industry in terms of cost. Historically, about $250 million are spent annually in the Gulf of Mexico and the North Sea due to stuck pipe troubles (Howard, J. A., & Glover, S. B. 1994). Stuck pipe is defined as the inability to pull out the drilling string due to downhole hitch. Commonly, there are two types of sticking pipe: mechanical sticking and differential sticking. Mechanical sticking covers several causes in the form of key seating, accumulation of drilling cutting due to inadequate hole cleaning, and borehole instability (caving and shale creeping).

Additionally, differential sticking occurs when there is a difference between the borehole pressure and the formation pressure. This difference tends to push the drilling string toward the formation, especially in front of permeable formations where mud cake is present. As a result, the drilling string will be embedded in the mud cake and the pipe unable to rotate and move up or down, but free circulation is easily retrieved. The stuck pipe problem is shown in Figure 1.5.

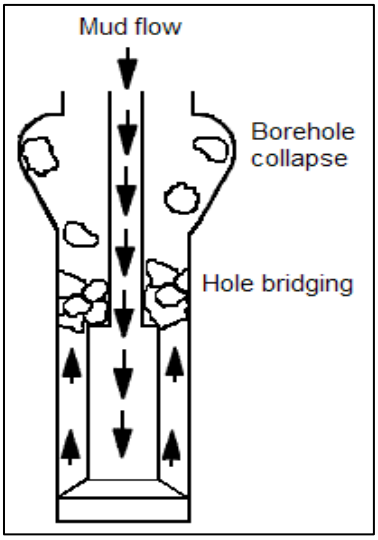

Figure 1.5.Stuck pipe

1.2. DATA UTILIZATION FOR WELLBORE STABILITY ANALYSIS

Various types of data for twenty vertical wells in the oil field southern Iraq were investigated in order to identify the wellbore stability problems and build a comprehensive geomechanical model. The following data were used in this analysis.

1.2.1. Daily Drilling Report. Several wellbore instability events were identified by using daily drilling reports. Problems such as stuck pipe, tight hole, and lost circulation were encountered while drilling a 12.25-in hole section. In general, the daily drilling report is a summary of daily drilling operations, and it is considered a helpful source in the prediction of the rock failure interval. This kind of report has a brief description of bottom hole assembly (BHA) profile and bit data in addition to information about the tripping and ream operations.

1.2.2. Daily Mud Reports. Daily mud reports were employed to estimate the mud characteristics, such as mud weight (MW), viscosity, yield point, and solid percent. Additionally, these daily mud reports described the daily losses as well as the cutting size.

1.2.3. Mud Logging Reports. Mud logging reports were used to predict the formation lithology of the interval of interest.

1.2.4. Final Well Reports. Final well reports were used to obtain the final productive time and NPT.

1.2.5. Well Logging Data. Well logging data such as sonic log, density log, and porosity log were employed to build a one-dimensional geomechanical model. Furthermore, image log and caliper log were used to identify the borehole breakout zone and the stress orientation. Pore pressure was predicted by using repeat formation test (RFT) for 20 wells.

1.3. GEOLOGICAL SETTING

Iraq is located in the northeastern part of the Arabian Peninsula and embraces the northwestern portion of the Arabian Basin and the Zagroes fold. Iraq has a complex geological setting with desert in the west and mountains in the North East. In geological terms, Iraq is positioned at the transition between the Arabian Shelf in the west and the intensely deformed Taurus and Zagros Suture Zones in the north and northeast. The Central depression of Iraq is categorized into south east part, which represents the Mesopotamia Plain, and the Jezira Plain in the northwest. The Jezira Plain located in the area between the Mesopotamian plain and the Euphrates depression of E Syria. The Mesopotamian plain (which is dominated in the southern part of Iraq) is bounded by the Euphrates River in the west and the Makhul-Hemrin-Pesh-i-Kuh range in the east. The geology of the Mesopotamian depression is produced by a complex system of river channels, levees, flood plain, marshes, sabkha and deltas, bordered on both sides by alluvial fans. Buday and Jassim (1987) pointed out that the Mesopotamian is located in the unstable shelf of the Arabian platform and classified it into three subzones. These subzones are the Tigris Subzone in the northeast, the Euphrates Subzone in the west, and the Zubair Subzone in the south of Iraq. In addition, Jassim and Goof (2006) mentioned that during the Hercynian deformation, the Mesopotamian was uplifted, then it subsided during the late Permian period.

Furthermore, the passive margin of Mesopotamian basin was formed by two tectonic phases, which are opening and closing phases (Numan, 2000). The opening phase illustrates the Permian-Jurassic period and represents the beginning of the Wilson cycle. The passive margin in the opening phase started forming when the Iranian and Turkish plates separated from the Arabian Plate. This separation caused an opening in the Neo-

Tethys Ocean. The closing phase was formed in the Cretaceous period and caused a reduction in the Neo-Tethys because the plates moved together. Later, the compressive forces on the passive margin lead to destroyed the rocks and formed oil traps. As a result, a reduction in the Mesopotamian passive margin has been formed.

According to Jassim and Goff (2006), the development of the Arabian Shelf was affected by the movement of the Precambrian basement and tectonism along the Neo Tethyan margin. The Arabian Plate is bounded by the passive margins in the west (which lies at the spreading ridges of the red sea) and Gulf of Aden in the south. The northern and northeastern boundaries are compressional due to the late tertiary collision of the Arabian Plate with the Turkish and Iranian Continents. Figure 1.6 shows the Arabian Plate in the present time. Some tectonic blocks of the Turkish and Iranian plates (now sutured to the Arabian Plate) were originally part of the Arabian Plate in Early-Mid Palaeozoic period. They later split off the Arabian Plate and became isolated microcontinents during the opening of the Neo-Tethys Ocean. In the Late Precambrian, the Arabian Plate joined the Indian and African Plates and formed part of Gondwana. At this time, the Northern Gondwana was subjected to an important period of tectonic extension. This extension created the NE-SE trending rift basins in southern Arabia (Husseini, 2002) and N-S trending grabens and half grabens in western and eastern Arabia (Andrews et al., 1991). Tectonically, the Arabian Plate is subducted under the Iranian and Anatolian Plates as a result of extensional movement.

The geology of Iraq has attracted the attention of researchers due to the abundance of hydrocarbons. In 2015, the Organization of the Petroleum Exporting Countries announced that the Iraq proven reserves reached to 142,503 (billion barrels). With this

reservation, Iraq had the second largest reserves in the Middle East and fourth in the world. Sharland et al. (2001) alluded that several tectonic periods formed the lithology succession in southern Iraq. This succession is called the Palaeozoic Megasequences. One of the important Palaeozoic megasequence is the late Tithonian-Early Turonian Megasequence, which is formed the middle part of the southern Iraq succession.

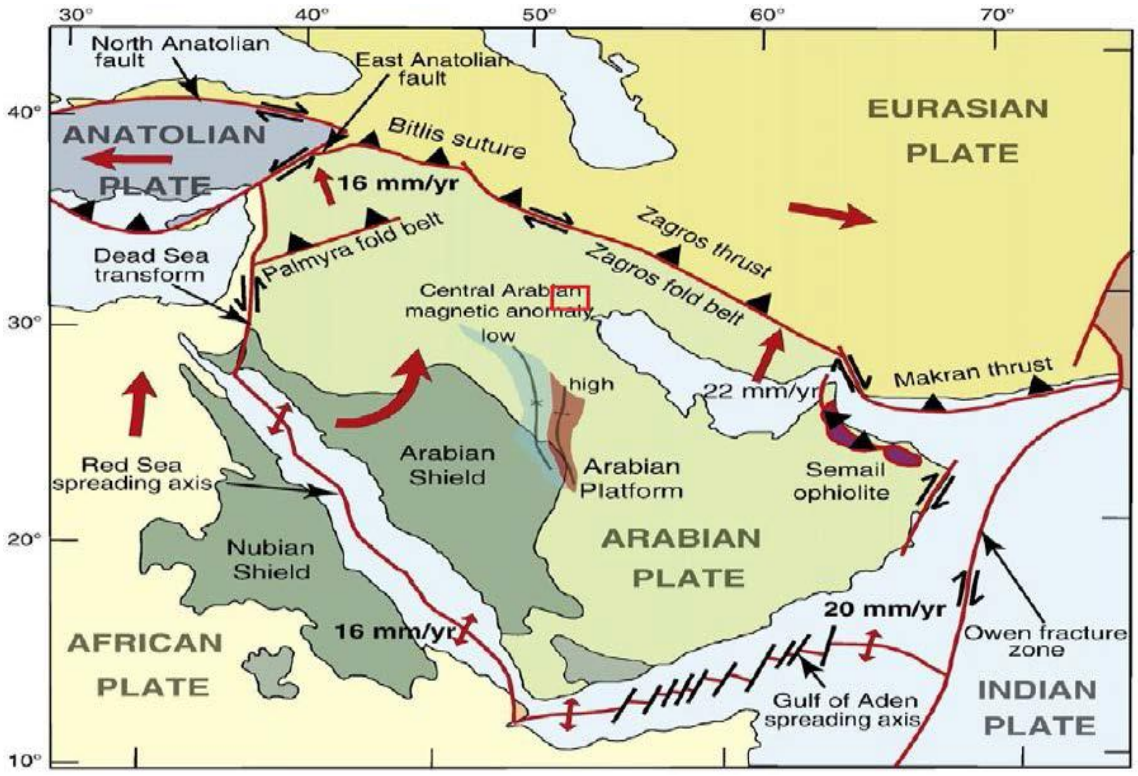

Figure 1.6. The Arabian Plate (Stern & Johnson, 2010)

The new Phase of ocean floor spreading in southern Neo Tethys was contemporaneous to the deposition of the Late Tithonian-Early Turonian Megasequence. This period was deposited in a large intra-shelf basin. The intra-shelf basin axis shifted from the Salman zone and western Mesopotamian zone to the eastern Mesopotamian zone into the Tigris subzone due to the differential subsidence that occurred across transverse

faults and the opening of the Neo-Tethys. Moreover, the Late Tithonian-Early Turonian Megasequence was comprised of four sequences: the late Tithonian-Hauterivian and Barremian-Aptian sequences (Thamama Group), and the Albian and Cenmanian-Early Turonian sequences (Wasi'a Group). During this sequences numerous formations were deposited in southern Iraq, such as Sulaiy, Yamama, Ratawi, Zubair, Shuaiba, Nahr Umr, and Mauddud. Nahr Umr Formation is the zone of interest and was deposited during the lower Cretaceous (upper Aptian-Albian) age, and it is well known due to its wide spread across Iraq (Figure 1.7) and for being a significant oil reservoir in southern Iraq (Jassim & Goff, 2006). Nahr Umr Formation is a sand-dominated clastic unit in the west and southwest and shale dominated toward the eastern parts of Iraq. In addition, the Nahr Umr Formation is a lateral equivalent of the Burgan Formation in Kuwait (Douban & Medhadi, 1999). In southwestern Iran, the formation passes into the shales and limestones of the Kazdhumi Formation (Furst, 1970). Additionally, it correlates with the Rutbah sandstone of the Palmyrides (Brew et al., 1999) and the Kurnub sandstone penetrated in Risha wells of northeastern Jordan.

Glynn Jones (1948) defined the Nahr Umr Formation based on Nahr Umr structure in southern Iraq. According to Bellen et al. (1959), the Nahr Umr Formation in southern Iraq is comprised of black shales interbedded with medium-to fine-grained sandstone with lignite, amber, and pyrite. Carbonate unit occurs locally in the upper part of this formation in southeastern Iraq. The average thickness of Nahr Umr Formation is +/- 260 m (Jassim & Goff, 2006). Its porosity ranges from 16 to 23%, and the permeability ranges from 20 to 3000 md (Aqrawi et al., 2010). The stratigraphic column of H oil field is shown in the Figure 1.8.

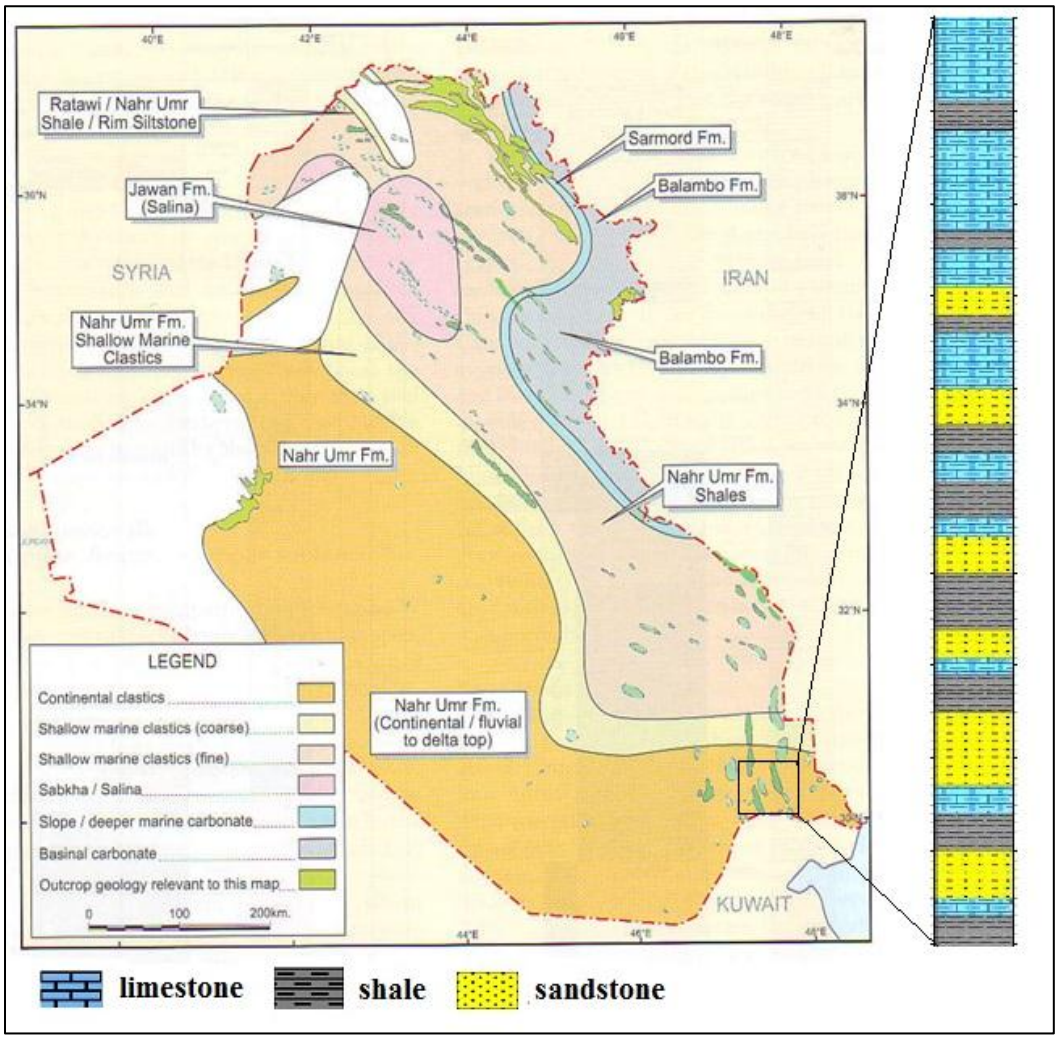

Figure 1.7. Geological map for Nahr Umr Formation (Aqrawi et al., 2010). The lithology bar on the right shows the rock types that comprise Nahr Umr formation in the study area.

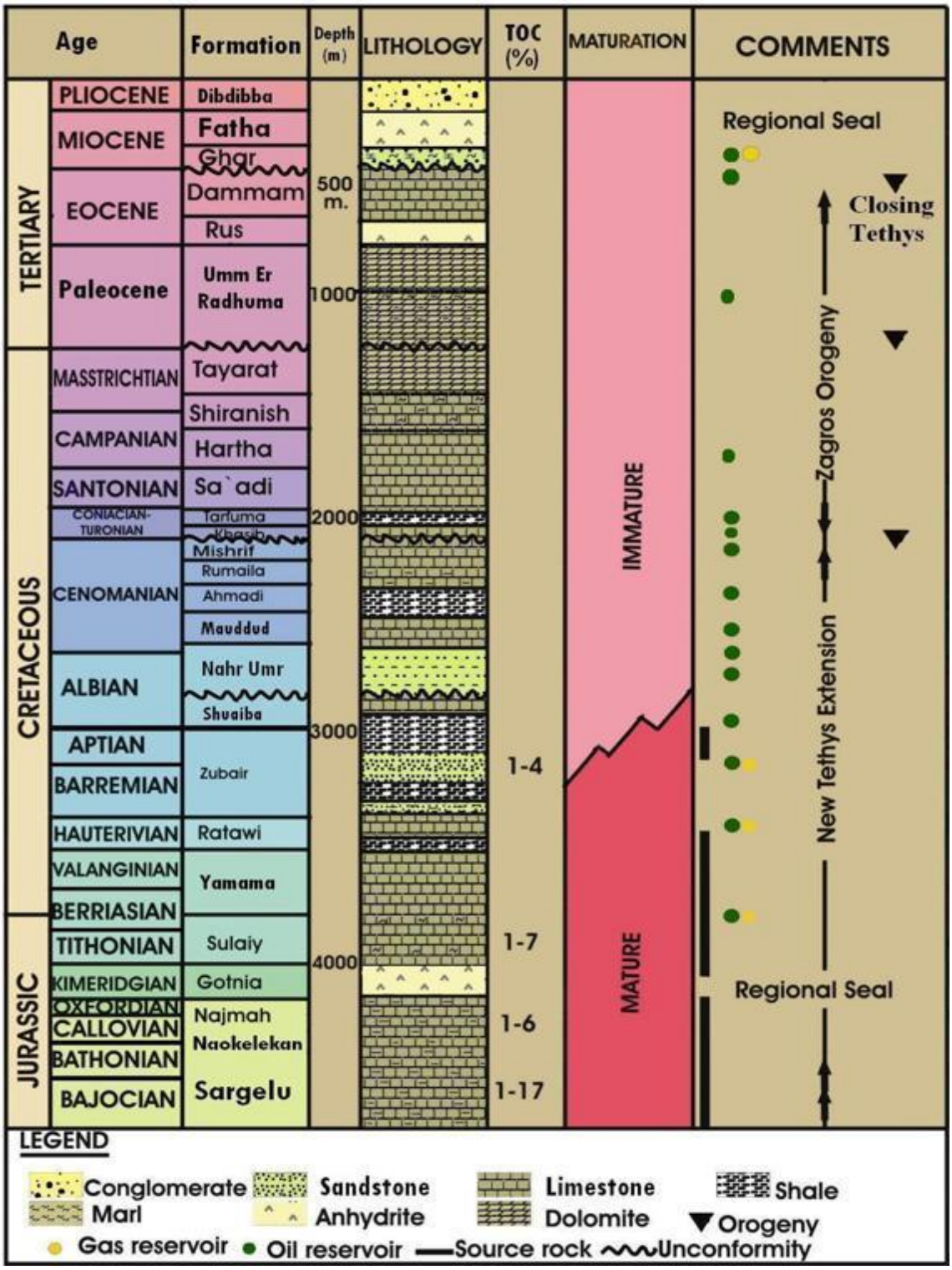

Figure 1.8. The stratigraphic column of H oil field.

1.4. LITERATURE REVIEW

A better understanding of borehole stability issues is necessary for drilling a well under difficult geological conditions. Wellbore instability in shale formation becomes one of the critical challenges that affect drilling operations. Problems related to wellbore instability are considered as time-and cost-consuming (Meng and Fuh, 2013). Therefore, wellbore failure has been studied extensively (Fjaer, 2008; Zoback, 2007). There are several factors that are associated with wellbore instability during drilling operation. These factors include, but are not limited to, mechanical-induced compaction, chemical effect, and well trajectory. Mechanical-induced compaction (mechanical failure) happens when the stress around the borehole exceeds the rock strength. On the other hand, chemical effect or fluid-rock interaction is another factor that leads to exacerbating the wellbore instability due to the reactivation between the drilling mud and the formation (especially shale). Additionally, some authors revealed that the weak bedding planes have a significant effect on the wellbore stability in an anisotropic formation (anisotropic rock strength can affect the stability of wells drilled at particular angles to the bedding planes). Thus, many studies are developed and implemented to eliminate/mitigate wellbore stability problems.

Bradly (1979) developed a theoretical model of the mechanical wellbore instability failure to predict hole breakout and induced tensile failure (hydraulic fracturing) and estimate optimum mud pressure to avert borehole failure. He pointed out that the model can be used in both vertical and directional borehole with a region under normal and tectonic conditions. His results show that the borehole inclination has a significant effect on the wellbore failure. For example, he found that the inclined wellbore will fracture by a pressure lower than that used in vertical one. Furthermore, he found that increasing wellbore inclination requires more mud pressure to prevent wellbore collapse. Also, the

results reveal that the borehole direction plays a major role in wellbore stability (especially in a tectonically active region).

Aadnoy and Chenevert (1987) studied the major wellbore instability failure mechanism by developing a linear elastic and isotropic model based on data from the U.S. Gulf Coast. The objective of their study was to understand the behavior of inclined boreholes in shale formation and create quantitative criteria. Their analysis used Von Mises and Mohr- Coulomb failure criteria. They found that the collapse failure is caused not only by shear failure but also by tensile failure, while fracturing is caused just by tensile failure. Furthermore, they pointed out that shear failure combined with tensile failure is the main reason behind the collapse failure in low borehole pressure. Additionally, they gave more weight on Mohr-Coulomb theory because it showed that the higher borehole inclination tends to be more sensitive to collapse, in contrast with Von Mises theory, which showed no increase in collapse sensitivity with increasing of borehole inclination.

Manshad et al. (2014) investigated the wellbore instability in the vertical, horizontal, and deviated wellbore by applying analytical and numerical methods for a well located in Iran. The objective of their study was to perform a comparison between four rock failure (namely, Mohr-Coulomb, Mogi-Coulomb, Modified Lade, and Tresca yield criterion) to estimate the optimum mud weight (to prevent wellbore collapse) and optimum drilling trajectory. Also, a finite difference method combined with an elastoplastic model has been used for mechanical wellbore stability analysis to show the validation and accuracy of the calculated mud pressure. The results illustrated that the Mogi-Coulomb and the modified Lade estimate the lowest minimum pressure, whereas the Mohr-Coulomb and Tresca criterion showed the highest minimum mud pressure. Furthermore, the minimum

mud pressure was obtained for a wellbore with an inclination of 20 degrees; the results indicate that the safest drilling direction for that inclination is at an azimuth of 90 degrees, which is the direction of minimum horizontal stress.

Yamamoto et al. (2002) studied the shale instability problems in Zakum field in Abo Dhabi. The study included a geomechanical and chemical view. Numerous field data were utilized, including drilling data, wireline logging, and well test data, and analysis of cutting and cores. Moreover, mineralogical tests and mechanical and chemical characteristics for the cutting and cores have been examined. The investigation showed that the shale has a severe mechanical strength and anisotropic physical features. Further, the authors concluded that the bedding plane failure is the main cause of wellbore instability in the laminated shale, and the drilling (mud chemistry) and formation fluid have a significant effect on wellbore instability in anisotropic and discontinuous shale.

Mansourizadeh et al. (2016) applied a comprehensive geomechanical model to estimate the in-situ and induced stresses. The purpose of this study was to predict the wellbore stability and breakout pressure via vertical and deviated well by utilizing failure criteria. The model has been constructed by employing several petrophysical, field data, and laboratory tests for one formation located in the southwest of Iran. Mohr-Coulomb (a 2D linear failure criterion), Hoek-Brown (a 2D nonlinear failure criterion), and Mogi-Coulomb (3D failure criterion) failure criteria were applied to estimate the breakout pressure. Stress transformation equations were used to investigate the effect of azimuth and inclination on the breakout pressure in the deviated wells. Their investigation illustrated that the Hoek-Brown criterion has more accurate results than the others. As a consequence of the sensitivity analysis that was performed for the inclination angle and the azimuth, the

authors concluded that the increase in wellbore inclination causes an increase in breakout pressure.

Waragai et al. (2006) presented an operation guideline to eliminate the severity of wellbore instability in the Nahr Umr shale formation in the offshore field in UAE after the prohibition of using the diesel in water-based drilling mud. A geomechanical model has been developed based on the mechanical and chemical analysis; these analyses were obtained by employing extensive field data such as open hole logging and core analysis. This study found that the Nahr Umr formation consists of laminated shale, the mechanical failure was imputed from the mud invasion into a lamination, and effective hole cleaning plays a major role especially with a hole angle between 30 and 50 degrees. As a result of the guideline implementation no well with sidetracking has been noticed. Based on the results they inferred that the guideline works and the wellbore instability problems can be mitigated by following it.

Ruzhnikov (2013) applied several steps to eliminate the shale instability of the production section in southern Iraq. These steps included constructing a geomechanical model to identify the main problems in the shale formation and find the possible root cause of these problems. Furthermore, core analysis, fracture development tests and cation exchange capacity (CEC) (to classify shale structure) were performed. Based on the analyses, Ruzhnikov proposed a new drilling fluid combined with good drilling practices to mitigate the shale instability. He also recommends using inhibitors and sealant components to prevent mud invasion into shale micro fractures and decreasing the exposure of formation to extravagant equivalent circulating density (ECD) by modifying the drilling strategy through shale formation.

Han et al. (2009) proposed modified drilling strategies after an investigation and ruled out the effect of the several wellbore instability mechanisms such us chemical reactions, weak beddings, and overpressure. In his analysis, he focused on fractured shale, which he considered as the main factor that causes the wellbore instability in Phu Horm field. Several tests have been conducted on a group of caving, includeing thin section, ultrasonic, and strength test. The investigation showed the tectonic movement causes an extensive fracture in the shale formation. Therefore, he concluded the shale instability problems at this area are combination of fractured shale and inappropriate mud weight. Finally, LCM and solids have to be added to the drilling mud to avoid mud penetration, mitigate swab, and surge operations. Redesign of the bottom hole assembly (BHA) has been recommended.

Alsubaih (2016) applied a geomechanical model to estimate the optimum mud pressure while drilling shale formations in southern Iraq. Data from 45 deviated wells have been examined to predict the majority of the non-productive time (NPT) in Tanuma shale formation. His study shows the most severe problem is stuck pipe, which is a result of wellbore shear failure.

Tutuncu et al. (2006) carried out a case study in terms of borehole stability and risk assessment in order to estimate optimum mud weight pressure. His analysis indicates that the key process in the success of well planning and avoiding wellbore stability problems (stuck pipe, lost circulation, and hole cleaning) is the identification of local and regional in-situ stresses in addition to formation lithology. Moreover, he mentioned that the in-situ stresses and rock strength properties were calculated by using sonic log and image log data along with drilling data. By using drill-cutting data, the hole cleaning parameters and well

trajectory were obtained. Furthermore, the study results have been implemented in the well design programs for the Amazon Jungle and show a good outcome in terms of reduction the amount of NPT. Finally, Tutuncu et al. concluded that the fluid pressures required for stable drilling decrease with hole inclination, which means the vertical well tends to use a higher mud pressure than the horizontal one.

2. THEORY OF ROCK MECHANICS

In well design, it is crucial to have a good understanding of rock mechanics. The design should consider several factors, including the influence of the fluid forces in the well and the formation pressure, seismic shock, and the thermal expansions/contractions. As well, overburden pressure has to be considered when drilling a deep well.

Solid engineering is designed under the concept of solid mechanics by employing analytical methods with adequate stiffness, strength, stability and integrity. Despite the high overlaps between the concepts and analytical methods of solid mechanics and continuum mechanics, solid mechanics are widely used across all branches of engineering and well design, including drilling, completion, and production (Aadnoy and Looyeh, 2011). There are two key components in solid mechanics: the internal resistance of an object that acts against the effect of external forces (denoted by stress) and the object deformation corresponding to external forces (represented by strain).

2.1. STRESS

In a simple definition, stress was introduced into the theory of elasticity as the force per unit area. This area could be an imaginary plane or a surface. Although calculating stress may be difficult (due to the amount of algebraic), knowledge about forces and tractions are required to understand the stress principles (Twiss and Moores, 2006). Stress is defined as

$$\boldsymbol{\sigma = \frac{F}{A}} \tag{1}$$

where σ is the stress (psi or pa), *F* is the force (N or lbf), and *A* is the area (M^2 or in^2).

Since the stress is the force acting on an area, it is therefore independent of the size and shape of the body. However, stress is dependent on the orientation. Going even further, there are two types of stresses resulting from the equilibrium condition, shown in Figure 2.1. These stresses are the normal stress (σ), which acts perpendicular to the plane, and the shear stress (τ), which acts along the plane.

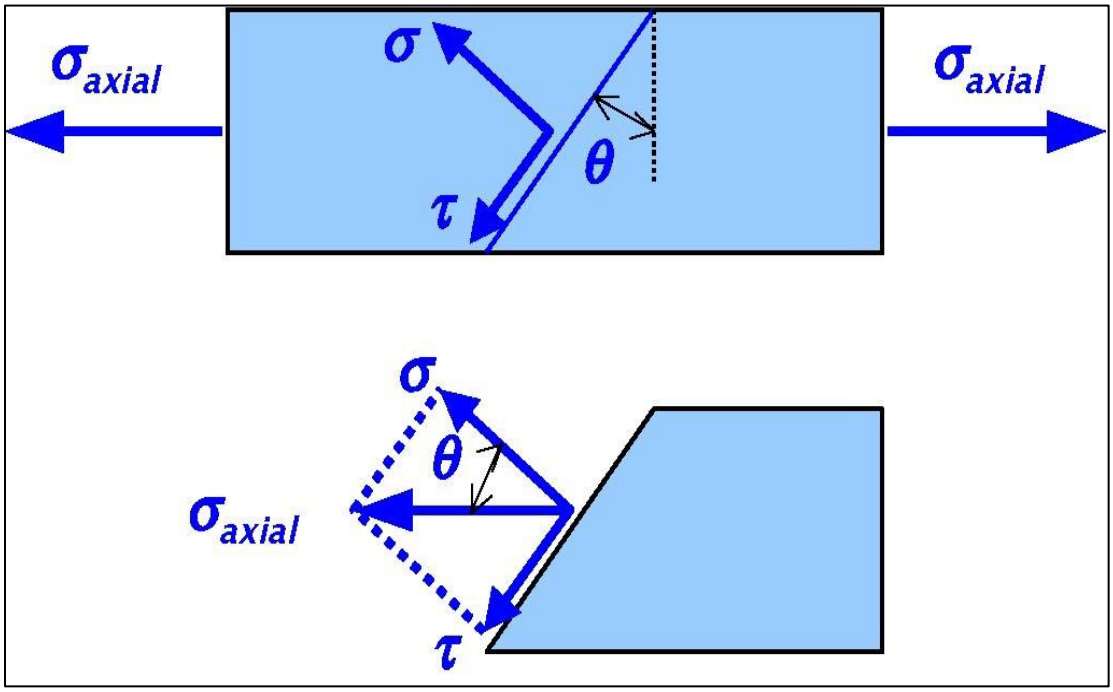

Figure 2.1. The normal stress and the shear stress (Aadnoy and Looyeh, 2011).

2.2. STRESS COMPONENTS

It is necessary to identify the stresses on the surface in a three-dimensional state to get a complete description of the state of stress at a point. Nine different components of stress are required to estimate the state of stress at a point, shown in Figure 2.2. The stress components are classified into two groups: normal stresses ($\sigma_{xx}, \sigma_{yy,}$ and σ_{zz}) and shear stresses ($\tau_{xy}, \tau_{xz}, \tau_{yx}, \tau_{yz}, \tau_{zx}$,and τ_{zy}).

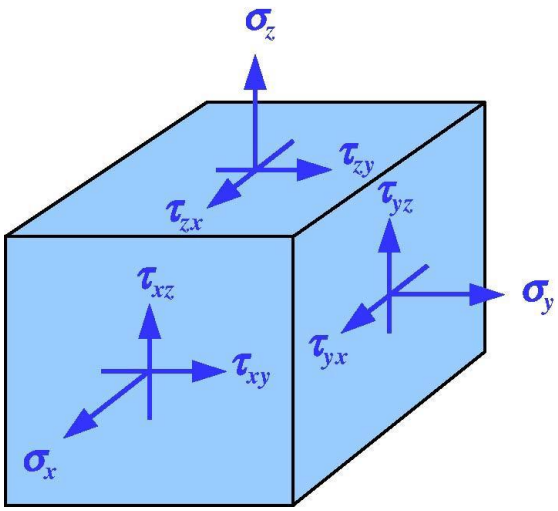

Figure 2.2. State of stress at three-dimensional (Aadnoy and Looyeh, 2011).

The first index in the alluded stress components described the axis normal to the plane on which the stress acts, while the second index illustrates the orientation of the stress component. The stress matrix of the nine stress components can therefore be expressed as

$$[\sigma] = \begin{bmatrix} \sigma_{xx} & \tau_{xy} & \tau_{xz} \\ \tau_{xy} & \sigma_{yy} & \tau_{yz} \\ \tau_{xz} & \tau_{yz} & \sigma_{zz} \end{bmatrix} \quad (2)$$

Equation 2.2 is known as stress tensor.

2.3. STRAIN

The body will undergo displacement and/or deformation as a result of shift and deformation when exposed to an external force. Therefore, any point in or out of the body will be displaced from its original position.

Aadnoy (2011) defined the strain as the ratio of the deformation to the original dimension. The strain is simply expressed by

$$\varepsilon = \frac{\Delta l}{l_o} \tag{3}$$

where ε is the strain, l_o is the original length (m or in), and Δl is the deformation dimension (change in length) (m or in.). This type of deformation is called elongation strain.

When the equation above is no longer valid (in the case of large deformation), two large deformations formulas introduced by Almansi and Green, respectively, can be used as follows:

$$\varepsilon = \frac{l^2 - l_o^2}{2l^2} \tag{4}$$

$$\varepsilon = \frac{l^2 - l_o^2}{2l_o^2} \tag{5}$$

2.4. ELASTICITY

Elasticity is the ability of a material to resist and recover from deformation after the external forces are gone. Many materials are subjected to the various types of forces. For instance, the formation rocks are exposed to in-situ stresses, pore pressure, and the drilling bit force. Therefore, knowledge about the rock characteristics is necessary to avoid any deformation and excessive failure. This knowledge is achieved by understanding of the stress-strain relationship.

The theory of elasticity is rests on the concept of stress and strain. Thus, it represents the linear relation between the applied force (stress) and the deformation produced by that force (strain) for the material which acts partially or entirely elastically.

Nevertheless, the stress-strain relation is not always linear due to the diversity of material properties and geometry.

2.5. HOOKE'S LAW

The linear relation between the stress and strain is known as Hooke's law and expressed by

$$\sigma_x = E\varepsilon_X \tag{6}$$

where σ_x and ε_X are defined in Equations 1 and 2, respectively, and E is the Young modulus or elastic modulus which is a measure of the rock stiffness. In other words, it is the resistance of the sample against the uniaxial stress. Young's modulus can be calculated from the slope of the stress-strain diagram as shown in the Figure 2.3 or by the triaxial and uniaxial compressive strength test in addition to empirical correlation.

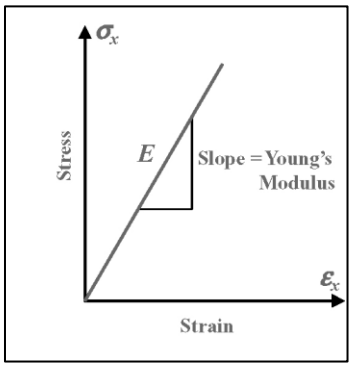

Figure 2.3. Stress-strain diagram

Lacy (1997) presented two empirical equation to estimate Young's Modulus, these equations are

$$Ed = 0.265vp^{2.04} \tag{7}$$

$$Es = 0.018Ed^2 + 0.422Ed \tag{8}$$

where E_d and E_s are the dynamic and static Young Modulus, and V_p is the compressive sonic wave.

2.6. POISSON'S RATIO

Poisson's ratio (ν) is one of the main mechanical properties used to estimate the wellbore stresses. This parameter is defined as the negative ratio of the lateral strain to the axial strain where ν is written as

$$\nu = -\frac{\varepsilon_y}{\varepsilon x} \tag{9}$$

In addition, many approaches compatible with well logging data have been developed to estimate the Poisson's ratio, such as

$$v = \frac{\frac{1}{2}\left(\frac{V_P}{V_S}\right)^2 - 1}{\left(\frac{V_P}{V_S}\right)^2 - 1} \tag{10}$$

where *v* is the Poisson's ratio, and *Vp* and *Vs* are the compressive and shear sonic wave (ft/ms).

2.7. IN-SITU STRESSES

Any point beneath the surface is subjected to three orthogonal principle stresses. These stresses are classified in terms of magnitude and orientation into vertical stress, minimum horizontal stress, and maximum horizontal stress. The in-situ stresses are generally nonhomogeneous, anisotropic, and compressive (Veatch and Moschovidis,

1986). Accordingly, in-situ stress plays a vital role in wellbore construction, planning, drilling, completion, production, and simulation of the well. Thus, it is important to have full knowledge about the in-situ stresses before performing any failure assessment and rock stress analysis. This knowledge could be helpful to understand and estimate the state of stress, predict the direction and the magnitude of the principle stresses, identify the directions of rock failure, determine the effect of the stresses on drilling and production operations, and investigate the main boundary in wellbore analysis (Aadnoy, 2011). Despite the significance of in-situ stresses, they have not received much attention. Therefore, the lack of data is recompensed by using indirect stress-related information (Avasthi et al., 2000).

Anderson (1951) proposed a fault regime classification for in-situ stress based on the ratio of horizontal stress magnitude to vertical stress magnitude. He assumed that no shear stress acts on the earth surface. Therefore, he described the normal or extensional fault (NF) as $S_V \geq S_H \geq S_h$, while the strike-slip fault (SS) and reverse fault (RF) regimes are associated with $S_H \geq S_v \geq S_h$ and $S_H \geq S_h \geq S_v$, respectively. Figure 2.4 illustrates the in-situ stress regimes. Moreover, Herget (1988) and Chen et al. (2002) presented the ratio of the maximum horizontal stress to minimum horizontal stress σ_H / σ_h as a range from 1 to 2 and σ_h / σ_v ranges from 0.3 to 1.5.

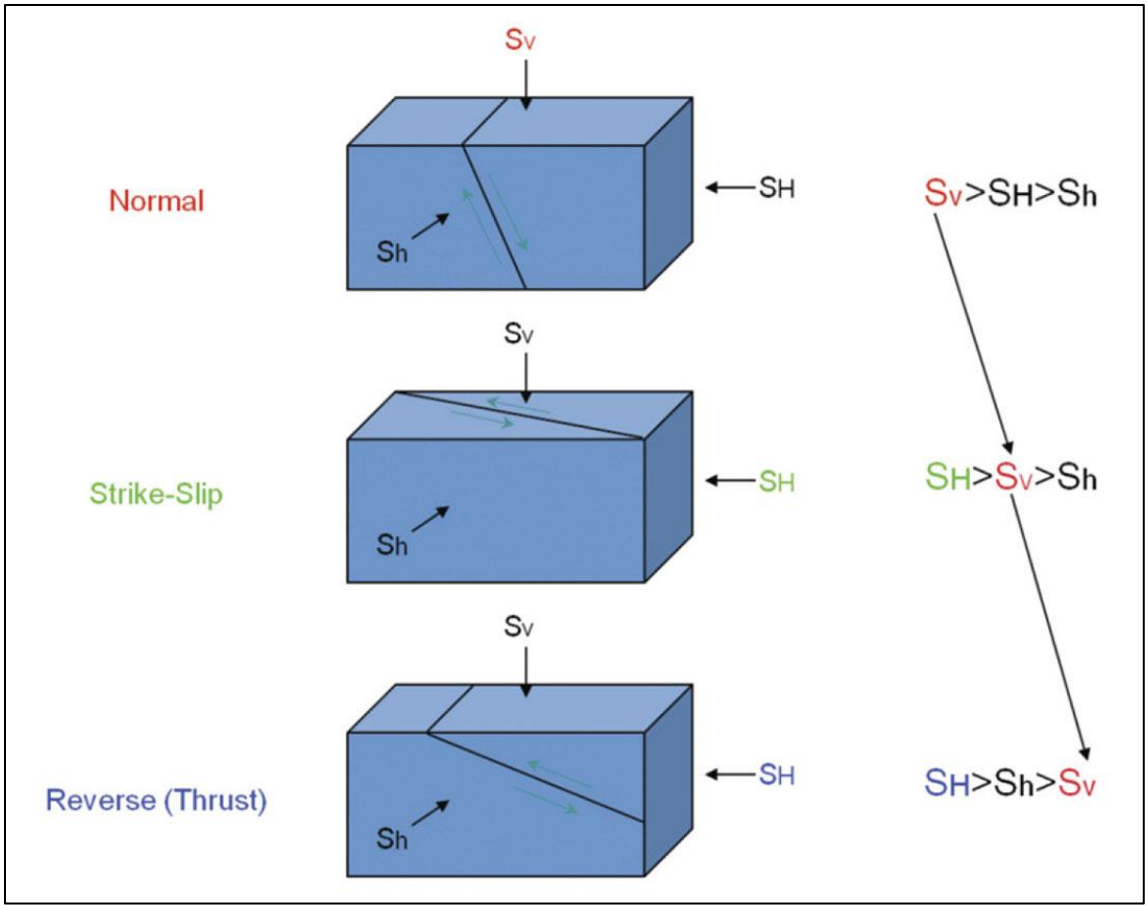

Figure 2.4. In-situ stress regimes (Wikel, 2011)

As illustrated in Figure 2.4, the vertical stress is dominated in the normal fault regime; the fault slip takes place when the minimum horizontal stress reaches a relatively lower value than vertical stress and pore pressure. When there is a significant difference between the maximum horizontal stress and minimum horizontal stress, a strike-slip fault will be created. On the other hand, the reverse fault is induced by the high diversity between maximum horizontal stress and vertical stress. Once both horizontal stresses exceed the vertical stress, a crustal shortening is accommodated throughout.

2.7.1. Vertical Stress. Vertical stress, also known as overburden stress, is the pressure imposed on a point by the weight of overlying formations. Overburden pressure has a direct propagation with the depth due to the increasing of sediments. The vertical stress of homogenous formation can be calculated by

$$S_v = \rho_a g z \qquad (11)$$

where ρ_a is the average density, g is the acceleration due to gravity, Z is the depth.

If the density varies with depth, the vertical stress can be estimated by the integration of rock densities as

$$S_v = \int_0^z \rho(z) g \, dz \qquad (12)$$

where ρ is the bulk density.

Among the many ways to calculate the bulk density, density logging tools have been used extensively (Bell 1990a). The bulk density at any point is considered as a combined of matrix density, fluid density, and the porosity of the formation, i.e.,

$$\rho_b = \rho_m (1 - \phi) + \rho_f \phi \qquad (13)$$

where ρ_m is the matrix density, ρ_f is the fluid density, and Ø is the porosity of the formation.

Density log is commonly not recorded at shallow depth. Therefore, many empirical approaches have been developed and used to obtained rock density at the shallow depth.

The vertical stress varies linearly with depth when the formations are cemented and well-compacted. The average density of sediments ranges between 1.8 and 2.2 g/cm3 and the overburden gradient 1 psi/ft (Fjaer et al., 2008).

2.7.2. Horizontal Stresses. Due to the effect of overburden pressure squeezing the rock vertically, the rock tends to move horizontally (Aadnoy, 2011). This movement has an impact on the horizontal stresses. In isotropic formation with no tectonic activities, minimum and maximum horizontal stress tends to be equal in value (i.e., when only overburden effect is present). When there are a major fault and tectonic activities, however, the horizontal stresses have different values and should be calculated. Hudson and Harrison (1997) summarized many direct approaches to estimate the horizontal stresses, including four testing techniques: the hydraulic fracture test, the flat jack test, the over-coring gauge test by the United States Bureau of Mines (USBM), and the over-coring gauge test by the Commonwealth Scientific and Industrial Research Organization (CSIRO).

However, national and international bodies suggested indirect methods to calculate the horizontal stresses; these approaches include acoustic emission, borehole breakouts, core discing, and differential strain analysis.

2.7.2.1 Minimum horizontal stress. Full knowledge of the orientation and magnitude of the horizontal stresses is necessary to find a solution for many geomechanics problems. Direct methods such as the leak off test (LOT), the extended leak off test (XLOT), and mini-frac. test can be used to obtain the minimum horizontal stress (Yamamoto, 2003; Zoback et al., 2003). Hydraulic fracturing is the most accurate technique for determining the minimum horizontal stress because it does not require the mechanical properties of the rock. The first use of hydraulic fracturing in stress measurement was in the 1960s (Haimson & Fairhurst, 1967). However, these tests are considered as time-and cost-consuming. Also, it is not routinely performed, and even when fulfilled, limited data set can be obtained. Consequently, leak off tests are widely

used to predict the minimum horizontal stress (Zoback et al., 1985) and the maximum mud pressure to prevent onset of the hydraulic fractures and assess the fracture gradient (Engelder, 1993; Jørgensen & Fejerskov, 1998). The LOT procedures are relatively simple, while the XLOT tests are more complicated because they include pressurizing producers. Practically, the leak off test is conducted after drilling (10-20 ft) below the last casing shoe. Once the test is carried out, the well is isolated and fluid (mud) is pumped into the well at a constant flow rate. Hence, the pressure is gradually increased, and a linear relation between the pressure and time is created as the volume of the borehole is fixed. The point where the pressure starts to diverge from the linearity is defined as the leak-off point (LOP) or fracture initiation pressure (FIP). Consequently, a hydraulic fracture is initiated. At this point and in the case of LOT, the pump is stopped as soon as the leak-off point has been clearly identified. However, the pumping will continue beyond the LOP point in case of XLOT, as shown in Figure 2.5. Hence, the pressure keeps increasing in a low rate until a distinctive pressure drop can be noticed. The pressure at this point is called formation breakdown pressure, and it represents the fracture propagation from the wellbore area (fluid will drain faster through the fracture more than the wellbore, thereby causing the pressure to drop). By keeping pumping with a constant rate, the pressure will then drop until it reaches a constant value, called the fracture propagation pressure (FPP). Finally, the pump is shut in, and the pressure drops. The instantaneous shut-in pressure (ISIP) is the pressure imposed on the wellbore when it is closed. ISIP is reported as a better measure of the minimum horizontal principle stress because at this point, any pressure associated with friction will vanish (Haimson &

Fairhurst, 1967). Additionally, if a viscous fluid is used, the FPP will increase. In such cases, the fracture closure pressure (FPP) will be the better measure of S_h.

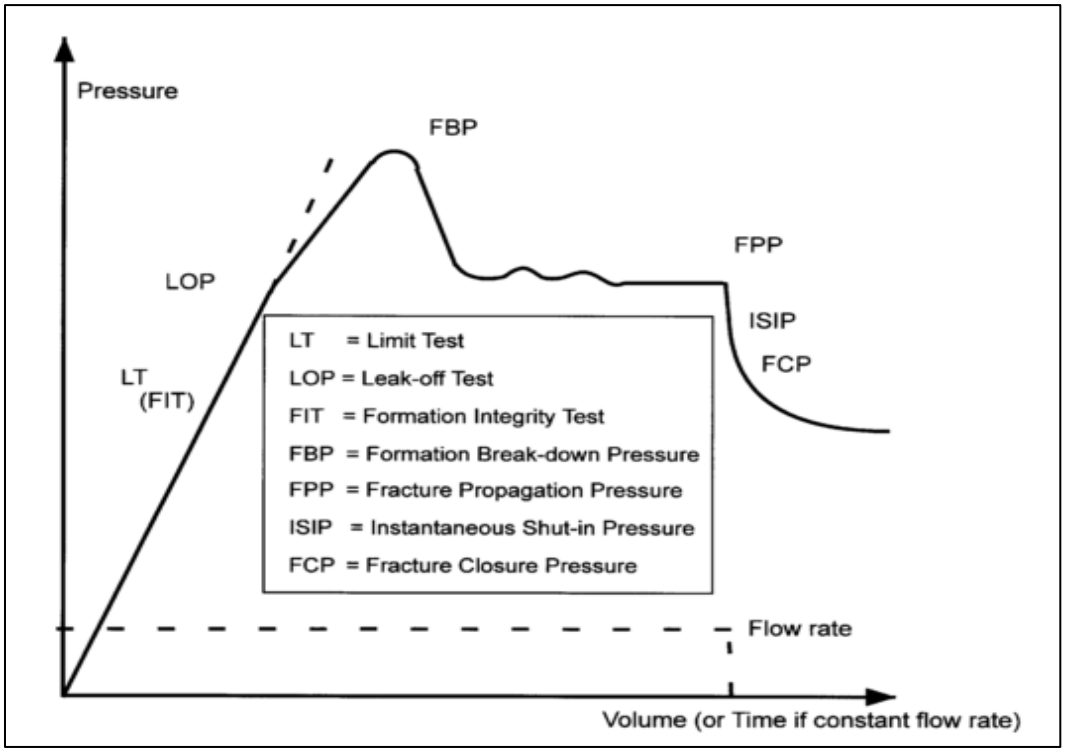

Figure 2.5. Formation strength tests (FIT, LOT, and XLOT).

Due to unavailability of the field tests, many empirical equations have been developed. Hubbert and Willis (1957) developed an empirical equation in the area of normal faulting such as the Gulf of Mexico to estimate the minimum horizontal stress as a function of vertical stress and pore pressure:

$$S_h = 0.3(S_v - p_p) + p_p \tag{14}$$

where P_p is the pore pressure, and 0.3 is a constant estimated by the hydraulic fracture data.

Eaton (1969) presented a modified version of the Hubbert and Willis approach; this method is derived from the bilateral constraint. He used a variable overburden stress gradient and a variable Poisson's ratio with depth. This approach is used to obtain the minimum horizontal stress of the Gulf Coast area, and it may be used in other areas.

$$S_h = \left(\frac{\upsilon}{1-\upsilon} \right) \left(S_v - p_p \right) + p_p \tag{15}$$

By 1982, Breckels and van Eekelen established empirical correlations to estimate the minimum horizontal stress as a function of depth. Hydraulic fracture data from different areas around the world were employed to derive these correlations. The correlations for the US Gulf Coast are

$$S_h = 0.0053Z^{1.145} + 0.46(P_p - p_h) \quad (\text{Z} < 3500 \text{ m}) \tag{16}$$

-

$$S_h = 0.0564Z - 31.7 + 0.46(P_p - p_h) \quad (\text{Z} > 3500 \text{ m}) \tag{17}$$

where P_h is the hydrostatic pore pressure.

Based on the frictional strength equilibrium concept, Zoback and Healy (1984) came up with newly derived equation after analyzing fluid pressure and in situ stress data from the Gulf Coast (Eq. 2.18). Lately, Holbrook (1990) proposed an empirical approach based on the porosity (Eq. 2.19). His techniques were based on a force-balance concept.

$$S_h = \left[\left(1+\mu^2\right)^2 + \mu\right]^2 * \left(S_v - p_p\right) + p_p \quad (18)$$

$$S_h = (1-\phi) * (S_v - p_p) + p_p \quad (19)$$

2.7.2.2 **Maximum horizontal stress.** The maximum horizontal stress is the most challenging parameter to estimate in the stress tensor accurately. There is no direct way to predict the value of maximum horizontal stress. As a result, many technical approaches have been developed. Addiset et al. (1996) proposed an equation based on the slippage on the fault by using the Mohr-Coulomb criterion and the theory of elasticity. Peng (2007) proposed an equation based on vertical stress, minimum horizontal stress, and fault regime (Eq. 20).

$$S_H = m * (S_v - S_h) + S_h \quad (20)$$

where S_H is the maximum horizontal stress and m is a constant.

2.8. PORE PRESSURE

Pore pressure is one of the main factors in geomechanical analysis and petroleum production. It has a significant effect on the wellbore stability analysis and the deformation around the wellbore (Detournay & Cheng, 1988). Therefore, pore pressure can be defined as the pressure induced by the formation fluid. The pore fluid can support part of overburden weight while the rest is carried out by the rock grains (Rabia, 1985).

Conceptually, the theory of pore pressure prediction relies on Biot's and Terzaghi's effective stress law (Biot, 1941; Terzaghi et al., 1996). This theory points out that pore pressure is a function of effective stress and total stress, i.e.

$$P_p = \frac{\sigma_T - \sigma_e}{\alpha} \tag{21}$$

where σ_T is the total stress, σ_e is the effective stress, and α is Biot's coefficient (α = 1, conventionally).

The inappropriate prediction of pore pressure can cause a significant NPT during the drilling and severe drilling incidents such as kick and blowout. Hence, several models have been developed to estimate the pore pressure (Standifird et al. 2004). Furthermore, well logs and direct measurements have been used to predict the pore pressure. Direct measurement is always applied in the permeable formations by using wireline technology such as repeat formation test (RFT) or via the pipe (drill stem test, DST, with packers to isolate the formation).

2.9. STRESS DISTRIBUTION AROUND THE WELLBORE IN VERTICAL WELLS

Underground formations undergo to vertical stresses caused by the weight of the overlying formation layers, and two horizontal stresses produced by the confining lateral restraints, the three stresses known as in-situ stresses. As a result of these in-situ stresses, the rock mass is in a balanced (static) state before drilling a borehole. Figure 2.6a demonstrates a schematic of stresses around a wellbore in a static state. This static state will be alerted and destroyed once the excavation is commenced. By commencing the drilling, the stresses are altered and changed due to rock removal; the load of these rocks

is carried out by the adjacent rock to readjust the equilibrium and to correspond with the new boundary condition at the wellbore. Therefore, the in-situ stresses are modified, as shown in Figure 2.6b. Due to the absence of the support pressure, failure at the borehole may occur. Maintaining pressure is required to prevent the onset of borehole failure; this pressure can be provided by a pressurized fluid called a drilling mud.

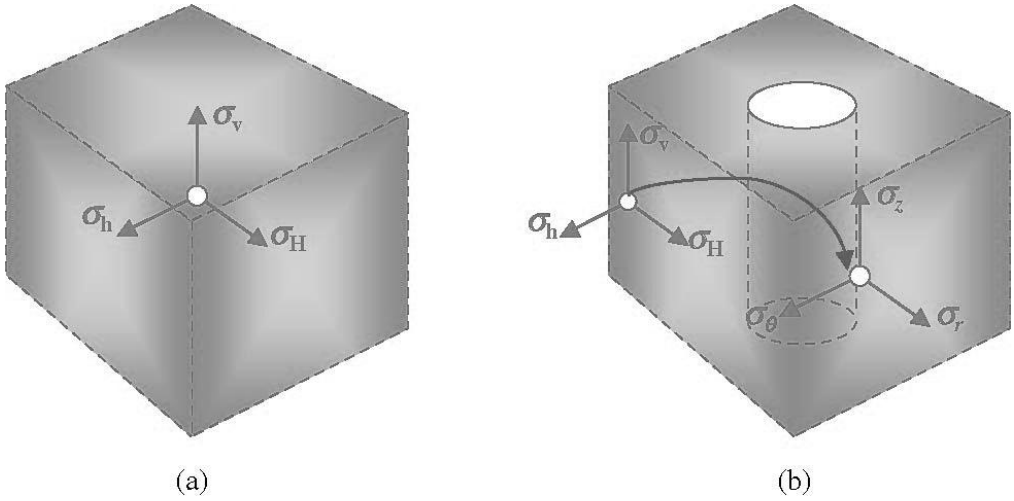

Figure 2.6. State of stress. a. State of stress at static state, b. State of stress at dynamic state.

A constitutive model is required to understand the stresses around a wellbore to estimate the possibility of mechanical instability at the borehole. Numerous models have been developed. Westergaard (1940) proposed an elasto-plastic model, which is considered one of the earliest works in the understanding of the stresses distribution around the borehole. Subsequently, many elasto-plastic models have been developed and presented, such as Gnirk (1972), Risnes and Bratli, (1981), Mitchell et al. (1987), and Anthony and Crook (2002). The requirement of using fewer input parameters encourages some authors

to present a new model. A linear elastic model has been established by Paslay and Cheatham (1963), Fairhurst (1965b), Bradley (1979), and Aadnoy (1989b).

Kirsch (1898) developed a solution for stress distribution around borehole in a cylindrical coordinate system. His analysis was built for the wells that were drilled perpendicular and parallel to the vertical stress (S_v) and was based on the assumption of linear elasticity, homogenous, isotropic, and elastic medium. The following equations were presented by Kirsch:

$$\sigma_r = \frac{1}{2}(\sigma_x + \sigma_y)(1 - \frac{a^2}{r^2}) + \frac{1}{2}(\sigma_x - \sigma_y)(1 + 3\frac{a^4}{r^4} - 4\frac{a^2}{r^2})\cos 2\theta + \tau_{xy}(1 + 3\frac{a^4}{r^4} - 4\frac{a^2}{r^2})\sin 2\theta + \frac{a^2}{r^2}p_w$$

$$\sigma_\theta = \frac{1}{2}(\sigma_x + \sigma_y)(1 + \frac{a^2}{r^2}) - \frac{1}{2}(\sigma_x - \sigma_y)(1 + 3\frac{a^4}{r^4})\cos 2\theta - \tau_{xy}(1 + 3\frac{a^4}{r^4})\sin 2\theta - \frac{a^2}{r^2}p_w$$

$$\sigma_z = \sigma_{zz} - 2\nu(\sigma_x - \sigma_y)\frac{a^2}{r^2}\cos 2\theta - 4\nu\tau_{xy}\frac{a^2}{r^2}\sin 2\theta \qquad (22)$$

$$\sigma_z = \sigma_{zz}$$

$$\tau_{r\theta} = \left[\frac{1}{2}(\sigma_x - \sigma_y)\sin 2\theta + \tau_{xy}\cos 2\theta\right](1 - 3\frac{a^4}{r^4} + 2\frac{a^2}{r^2})$$

$$\sigma_{rz} = (\tau_{xy}\cos\theta + \tau_{yz}\sin\theta)(1 - \frac{a^2}{r^2})$$

$$\sigma_{\theta z} = (-\tau_{xz}\sin\theta + \tau_{yz}\cos\theta)(1 + \frac{a^2}{r^2})$$

where σ_r is the radial stress, which acts along the radius of the wellbore, σ_θ is the hoop stress acting tangential to the wellbore, σ_z is the axial stress which acts parallel to the well path and tangential too, *a* is the wellbore radius, p_w is the drilling mud pressure, and ν is Poisson's ratio. The angle θ is measured clockwise from the x-axis.

By assuming of the anisotropic solution and r = a, Kirsch's equations are defined the following:

$$\sigma_r = p_w$$

$$\sigma_\theta = \sigma_x + \sigma_y - p_w - 2(\sigma_x - \sigma_y)\cos 2\theta - 4\tau_{xy}\sin 2\theta$$

$$\sigma_z = \sigma_{zz} - 2\nu(\sigma_x - \sigma_y)\cos 2\theta - 4\nu\tau_{xy}\sin 2\theta$$

$$\sigma_z = \sigma_{zz} \tag{23}$$

$$\tau_{r\theta} = 0$$

$$\tau_{rz} = 0$$

$$\tau_{\theta z} = 2(-\tau_{xz}\sin\theta + \tau_{yz}\cos\theta)$$

By changing the stresses corresponding to effective principle stress at the wellbore, the equations will be defined as

$$\sigma_r = p_w$$

$$\sigma_\theta = (\sigma_H + \sigma_h) - 2(\sigma_H - \sigma_h)\cos 2\theta - p_w \quad (24)$$

$$\sigma_z = \sigma_v - 2\nu(\sigma_H - \sigma_h)\cos 2\theta$$

2.10. STRESS POLYGON

It is helpful to consider that the values of the three principle stresses in the form of S_v, S_H, and S_h relies on the method that proposed by Anderson (1951). Zoback et al. (1986) introduced a new method to constrain stress magnitudes called stress polygon. This method was derived based on the definition of Coulomb's theory for faulting and Anderson's faulting theory.The polygon technique allowed a range of possible stress magnitudes to be predicted for a point at a particular depth for a given pore pressure and assumed friction's coefficient. Figure 2.7 shows the main construction of the stress polygon as a function of σH and σh. Additionally, the stress polygon figure demonstrates an allowable range of magnitudes for the minimum and maximum horizontal stress in case of three fault regimes (NF, SS, RF). The value of the two horizontal stresses was found by using one of the equations below:

For normal fault:

$$\frac{\sigma_1}{\sigma_3} = \frac{S_v - p_p}{S_{h.} - p_p} \leq \left[\left(\mu^2 + 1\right)^{1/2} + \mu\right]^2 \quad (25)$$

For strike-slip fault:

$$\frac{\sigma_1}{\sigma_3} = \frac{S_H - p_p}{S_h - p_p} \leq \left[\left(\mu^2 + 1\right)^{1/2} + \mu\right]^2 \quad (26)$$

For reverse fault

$$\frac{\sigma_1}{\sigma_3} = \frac{S_H - p_p}{S_v - p_p} \leq \left[\left(\mu^2 + 1\right)^{1/2} + \mu\right]^2 \tag{27}$$

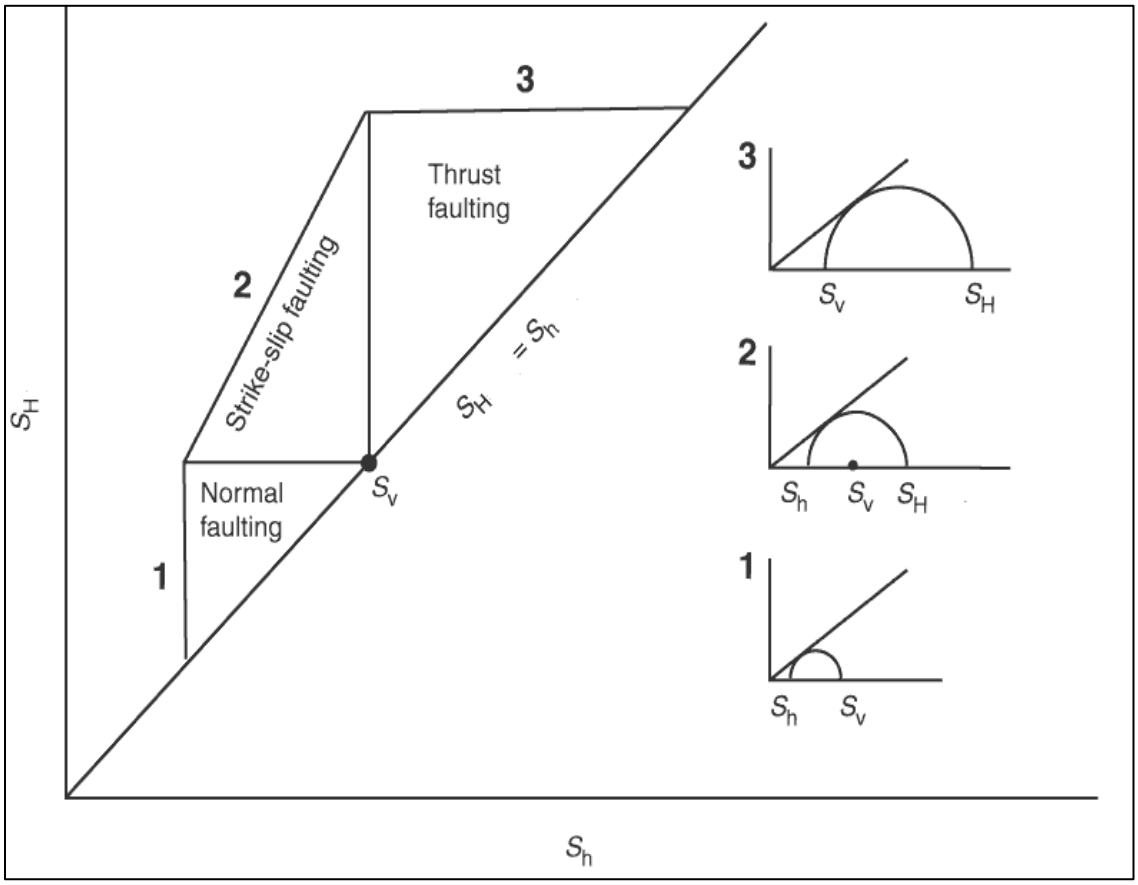

Figure 2.7. Stress polygon (Zoback et al., 2003).

2.11. ROCK STRENGTH PROPERTIES

Rock strength parameters play a crucial role in petroleum-related geomechanics. Compressive and tensile strength, including unconfined compressive strength (UCS), tensile strength, cohesion, and internal friction angle, are considered the key processes in any wellbore stability analysis. These parameters can be calculated by means of core sample tests (Peng et al., 2002a). However, the core samples are not available in most cases

especially in the deep wells, and these cores are just from a small segments of the well interval. So, direct measurements such us uniaxial and triaxial strength tests can be used. Therefore, well logging data are employed with compatible correlations to estimate the rock strength parameters for the entire section. These correlations have been derived for specific rock formations that rely on the relationships of geophysical data and core tests.

2.11.1. Cohesion. Cohesion, or cohesive strength, is defined as the ability of the molecules to stay connected with each other. Moreover, when there is no applied normal stress, cohesion will represent the shear strength of the rock (Aadnoy & Looyeh, 2001). Cohesion is described base on the Tresca criterion as

$$S_o = \tau_{max} = \frac{1}{2}(\sigma_1 - \sigma_3) \tag{28}$$

where S_o is the cohesion (inherent shear strength), and σ_1 and σ_3 are the maximum and minimum principle stress respectively (Fjaer et al., 2008).

In a Mohr-Coulomb plot, the Tresca criterion looks like a straight horizontal line, as shown in Figure 2.8.

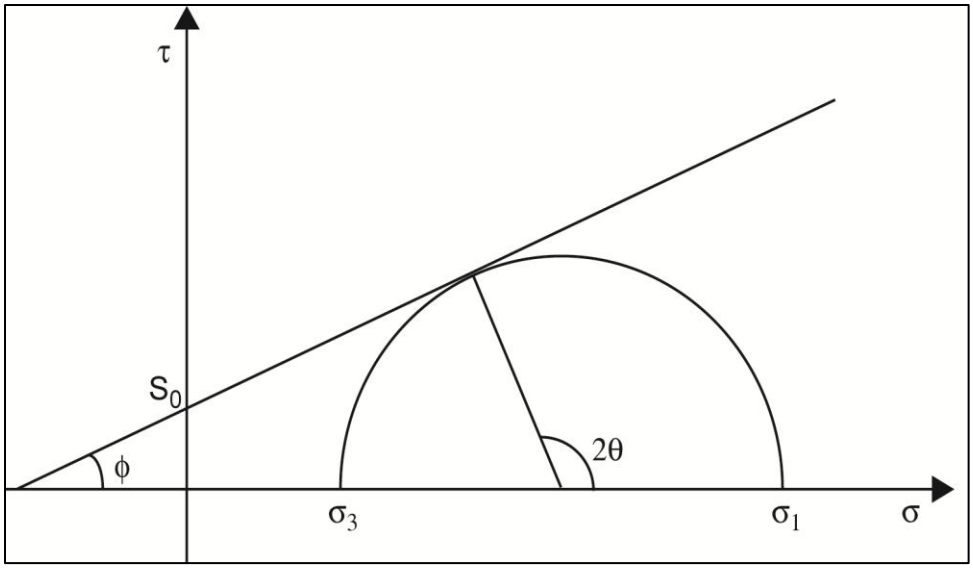

Figure 2.8. Mohr-Coulomb criterion

2.11.2. Internal Friction Angle. Internal friction angle, which represents the ability of the rock to resist the shear failure, is an important parameter in predicting the rock failure. So, Friction angle (φ) is defined graphically based on the Mohr-Coulomb criterion plot as the angle of inclination with respect to the normal stress (horizontal axis). Recently, numerous studies on the relationship between the friction angle and rocks stiffness have been conducted due to the variety of rock behaviors (some weak rock shows high value of friction angle). Lama and Vutukuri (1978) reveal that shales with high Young's modulus tend to present a high value of φ. In order to meet the needs, methods such as core lab analysis and special rock tables can be used to obtain the friction angle (Zoback, 2010). In addition, several empirical equations were developed due to the absence of core sample. A correlation conducted by Plumb (1994) was derived as a function of porosity and shale volume as

$$\varphi = 26.5 - 37.4(1 - NPHI - V_{Shale}) + 62.1(1 - NPHI - V_{Shale})^2 \quad (29)$$

Where φ is the friction angle, *NPHI* is the porosity from neutron porosity log, and V_{shale} is the shale volume which is expressed by

$$V_{Shale} = \frac{GR - GR_{\min}}{GR_{\max} - GR_{\min}} \quad (30)$$

where *GR* is the value of gamma ray log, and GR_{max} and GR_{min} are the maximum and minimum values of gamma ray log, respectively.

2.11.3. Unconfined Compressive Strength. Rocks tend to fail when the compressive shear strength exceeds rock strength. This exceeding can lead to mechanical failure in the wellbore. Mechanical failure in the rock means either fracturing or permeant deformation in the wellbore has occurred as a result of compression. The unconfined compressive strength (UCS) is one of the key parameters in rock strength. Several methods gave been used to estimate UCS, including direct and indirect methods. The uniaxial compression test has been widely used as a direct measurement and is considered one of the key loading tests performed on rocks to predict UCS. This test is applied base on the American Society for Testing and Materials (ASTM) D 5102-09 standard. Pariseau (2006) reported that rock specimens usually fail by fracture under the unconfined compression test.

However, due to the absence of core samples for laboratory testing, many empirical correlations between rock strength and well logging data have been developed (Peng et al., 2001). Chang (2006) has summarized several empirical correlations for a different kinds of formations, sandstone (Vernik et al., 1993), shale (Lal, 1999), and limestone (Middle East) to predict the unconfined compressive strength:

For shale

$$UCS = 10\left(\frac{304}{(\Delta t - 1)}\right) \tag{31}$$

For limestone

$$UCS = 143.8 * \exp(-6.95 * \phi) \tag{32}$$

For sandstone

$$UCS = 254(1 - 2.7\phi)^2 \tag{33}$$

where Δ_t is the sonic slowness (μs/ft) and ϕ is the rock porosity.

2.12. ORIENTATION OF PRINCIPLE HORIZONTAL STRESSES

The orientation of the principle stresses is an essential aspect in wellbore failure analysis (Barton et al., 1997). Zoback et al. (2003) pointed out that in the area of maximum hoop stress, the wellbore is most likely to be under compressive failure (at the S_h azimuth). Zoback et al. (1985) defined the orientation of the maximum horizontal stress as perpendicular to the breakout direction.

2.13. ROCK FAILURE CRITERIA

Rock failure occurs when the stresses surrounding the wellbore exceed one of the allowable strengths of the rock (tensile, compressive, or shear strength). Therefore, designing an appropriate mud window by using compatible rock failure criteria plays a significant role in wellbore stability. Since there is no specific failure criterion works with all material and cases, several failure criteria have been developed to predict rock failure based on types of rock failure and lithology. These criteria mimic the behavior of the stresses around the wellbore. In any analysis, it is essential to select appropriate criteria for

a given problem. This selection is based on the types of the rocks (ductile or brittle). The objective of using the failure criterion is to determine the suitable mud windows to prevent failure. Further, it applies a comparison between the internal stresses with the strength of the material. In general, failure criterion is used to predict the safe wellbore trajectory (identify the stable and unstable regions in drilling) and optimum mud window.

2.13.1. Mohr-Coulomb Failure Criteria. Mohr-Coulomb shear failure criterion is the most frequently used criteria in mechanical earth modeling due to its simplicity (Horsrud, 2001; Fjaer et al., 2008). In this failure criteria, shear failure takes place through a plane due to the effect of shear stress on that plane. Additionally, Mohr failure criterion is considered as a 2D linear approach because it assumes that the intermediate principle stress has no influence on rock strength. As a result, Mohr-Coulomb is expected to be deficient and conservative in estimating the optimum mud window because the intermediate principle stress may feed rock with additional strength. The linearized form of the Mohr failure criterion is expressed as

$$\tau = c + \tau_n \tan \phi \tag{34}$$

where τ is the shear stress, *c* is the rock cohesion, τ_n is the normal stress, and ø is the internal friction angle.

The coefficient of internal friction angle can be formulated as

$$\mu = \tan \phi \tag{35}$$

Mohr failure criteria can also be expressed by the maximum and minimum principle stresses, as follows

$$\sigma_1 = c_o + q\sigma_3 \tag{36}$$

where σ_1 and σ_3 are the maximum and minimum principle stresses, repectivily. c_o, is the unconfined compressive strength, which is a function of cohesion and internal friction angle and q is the flow factor, which is related to internal friction angle and can be obtained by

$$q = \frac{1 + \sin\phi}{1 - \sin\phi} \tag{37}$$

$$c_o = 2c\frac{\cos\phi}{1 - \sin\phi} \tag{38}$$

2.13.2. Mogi-Coulomb Failure Criteria. Mogi (1971) implemented laboratory studies on different types of rock by using a triaxial compression techniques. He found that the strength of the rock is markedly affected by the magnitude of intermediate principle stress and the fracture occurs along the direction of σ_2. Based on his observation, Mogi came up with new criterion that takes into account the effect of intermediate principle stress. Moreover, Mogi alluded that ($\sigma_{m,2}$) is the mean normal stress that opposes the creation of the fracture instead of the normal octahedral stress (σ_{oct}):

$$\sigma_{m,2} = \frac{(\sigma_1 + \sigma_3)}{2} \tag{39}$$

$$\sigma_{oct.} = \frac{1}{3}(\sigma_1 + \sigma_2 + \sigma_3) \tag{40}$$

Therefore, Mogi suggested new criteria, defined as

$$\tau_{oct} = f(\sigma_{m,2}) \tag{41}$$

where the octahedral shear stress is expressed as

$$\tau_{oct.} = \frac{1}{3}\sqrt{(\sigma_1 - \sigma_2)^2 + (\sigma_2 - \sigma_3)^2 + (\sigma_3 - \sigma_1)^2} \tag{42}$$

After this observation, it became obvious the importance of σ_2. Therefore, many 3D failure criteria have been developed. After performing extensive reviews of rock failure models, Al-Ajmi and Zimmerman (2005) introduced a 3D failure criterion called the Mogi-Coulomb criteria. This criterion can be formulated as a linear relation in a similar format to the Mohr-Coulomb criterion as follows:

$$\tau_{oct} = a + b\sigma_{oct} \tag{43}$$

Where *a* and *b* are material constant and are related to *c* and *ø* as follow

$$a = \frac{2\sqrt{2}}{3} c \cos\phi \tag{44}$$

$$b = \frac{2\sqrt{2}}{3} \sin\phi \tag{45}$$

2.13.3. Modified Lade Failure Criteria. Lade (1984) proposed 3D failure criteria that considered the effect of intermediate principle stress. This approach was initially proposed for frictional materials without effective cohesion. Fourteen years later, Ewy (1999) further developed the Lade criteria and proposed the modified Lade criteria. In modified Lade criteria, only two rock strength parameters are required: cohesion and friction angle (Zoback, 2007). The modified Lade criterion is given as

$$\frac{I_1^{'}}{I_3^{'}} = 27 + \eta \tag{46}$$

where I_1' and I_3' are stress invariants and are defined as

$$I_1^{'} = (\sigma_1 + s) + (\sigma_2 + s) + (\sigma_3 + s) \tag{47}$$

$$I_3^{'} = (\sigma_1 + s) + (\sigma_2 + s) + (\sigma_3 + s) \tag{48}$$

s and η are material constants, where *s* is related to the cohesion of the rock and η represents the internal friction. These parameters can be derived directly from the Mohr-Coulomb cohesion (S_o) and internal friction angle (ϕ) by

$$S = \frac{S_0}{\tan \varphi} \tag{49}$$

$$\eta = \frac{4 \tan^2 \varphi (9 - 7 \sin \varphi)}{1 - \sin \varphi} \tag{50}$$

where tan $\varphi = \mu i$ and $S_0 = C_0/ (2\ q1/2)$ with q defined by $q = tan^2 (\frac{\pi}{4} + \frac{\emptyset}{2})$.

3. DATA AND ANALYSIS

3.1. DATA SOURCE

Data from twenty vertical wells are examined to detect the majority of the wellbore instability problems. This data included field tests, such as the extended leak off test (XLOT), and well logging (gamma ray, caliper, density, sonic, and porosity). The investigation reveals that the majority of the wells have suffered from sticking pipe, caving, and tight-hole problems, and one well with sidetrack was noticed.

3.2. GEOMECHANICAL MODELS FOR NAHR UMR FORMATION

From theoretical to experimental aspects, a comprehensive model on the mechanical effects on wellbore stability in the Nahr Umr Formation for a field located in southern Iraq was considered in this study. The process of building a geomechanical model implies the prediction of the elastic and mechanical properties from physical equations and correlations (Zoback, 2007; Aadnoy, 2010). Then, the magnitudes of three principle stresses (vertical stress, minimum horizontal stress, and maximum horizontal stress) and pore pressure are to be calculated. Therefore, pore pressure, rock mechanical properties, and in-situ stresses are considered among the main factors for building a geomechanical model. In this study, four wells were selected based on the location of the wells according to H field domes.

3.3. THE ORIENTATION OF HORIZONTAL STRESSES

The orientation of the horizontal stresses was estimated by performing image interpretation analysis on the STAR image log acquired from Well H-50. According to Zoback et al. (1985), breakout orientation is created along the direction of the minimum horizontal stress. Figure 3.1 shows three breakout zones with a combined length of 15 m.

In addition, it can be noticed that the breakout orientation ranges between 135-140°. Therefore, the direction of the maximum horizontal stress is between 45-50°.

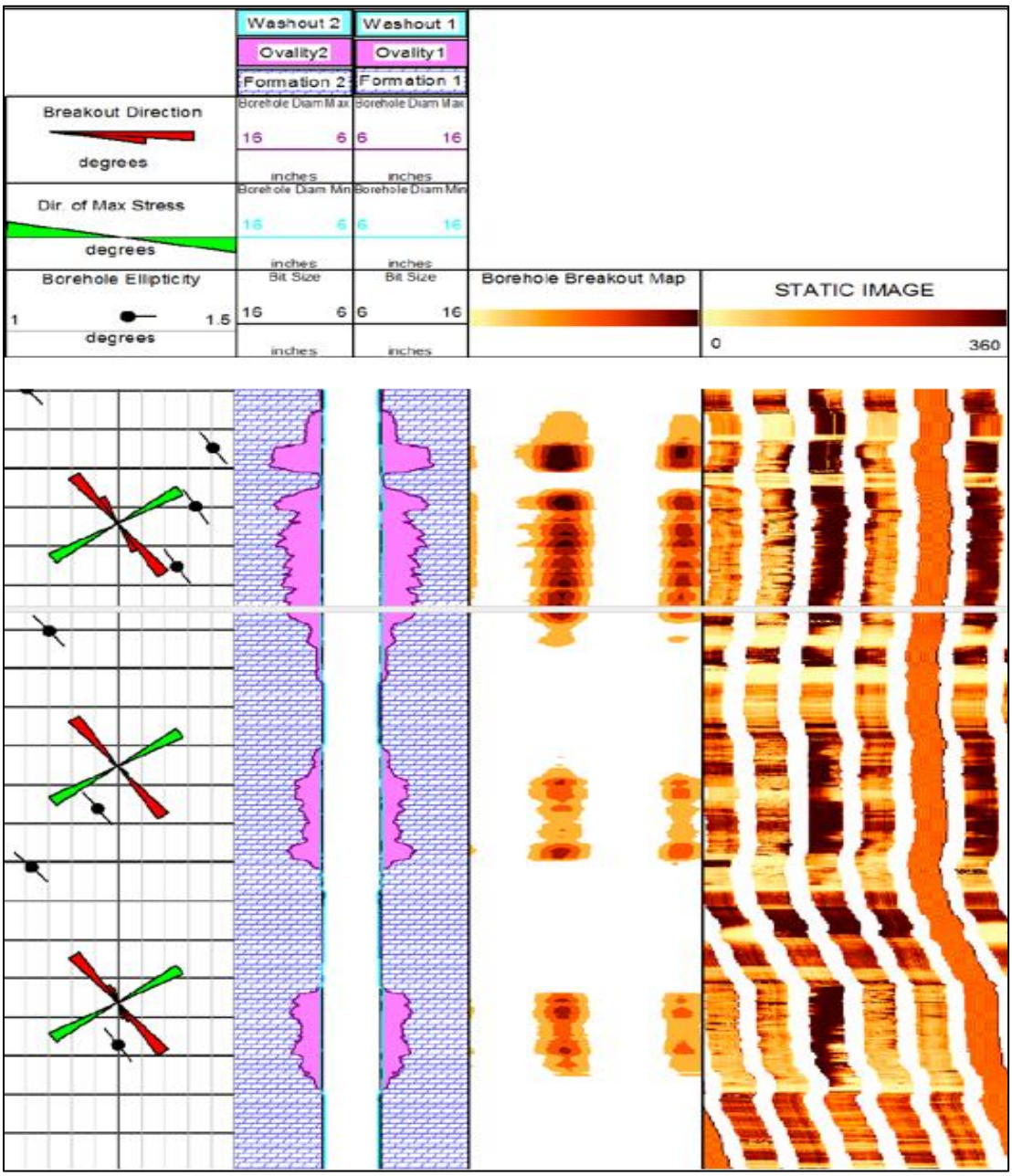

Figure 3.1. Star image log shows the breakout zone within well H-50.

3.4. CASE STUDY 1

The well H-10 is part of H Field Development Plan; its objective is to produce oil from 3rd pay Reservoir in the northern part of the field. The H Field is one of the mature oil fields in southern Iraq. It is located 20 km southwest of Basra city. The 12.25-in. hole of well H-10 was drilled with KCl Polymer mud type, and the mud weight ranged from 1.18 to 1.24 Sg. This section drilled through Sadi, Tanuma, Khasib, Mishrif, Rumaila, Ahmadi, Maddud, Nahr Umr, Shuaiba, and few meters in Zubair upper shale formation. Severe loss rates up to 40 m^3/hr have been encountered while drilling at a depth of 2252 m (Mishrif formation). Therefore, a cement plug was used to stop the losses. Moreover, several drag and tight spots were faced at Nahr Umr Formation, and caving was noticed on the shale shaker. The lithology description of Nahr Umr Formation in the well H-10 was presented as

1- Limestone: Wackstone, packstone, dark grey, grey, soft to moderately hard, sub blocky to blocky, fine crystalline, argillaceous, no visual porosity, no oil show.
2- Shale: Dark grey, grey, brownish grey, firm to moderately hard, fissile, non-calcareous.
3- Sandstone: Quartz, light brown, white, transparent to translucence, fine grain, sub rounded to rounded, moderately hard, well sorted, calcareous cement, no visible matrix, poorly visible porosity, no oil shows.

The construction procedure of the mechanical earth modeling in well H-10 is given below.

3.4.1. Pore Pressure. Pore pressure is one of the important parameters that has a significant effect on wellbore stability. Pore pressure was directly calculated by utilizing the repeat formation test (RFT). Figure 3.2 shows the variation of the pore pressure with respect to the depth.

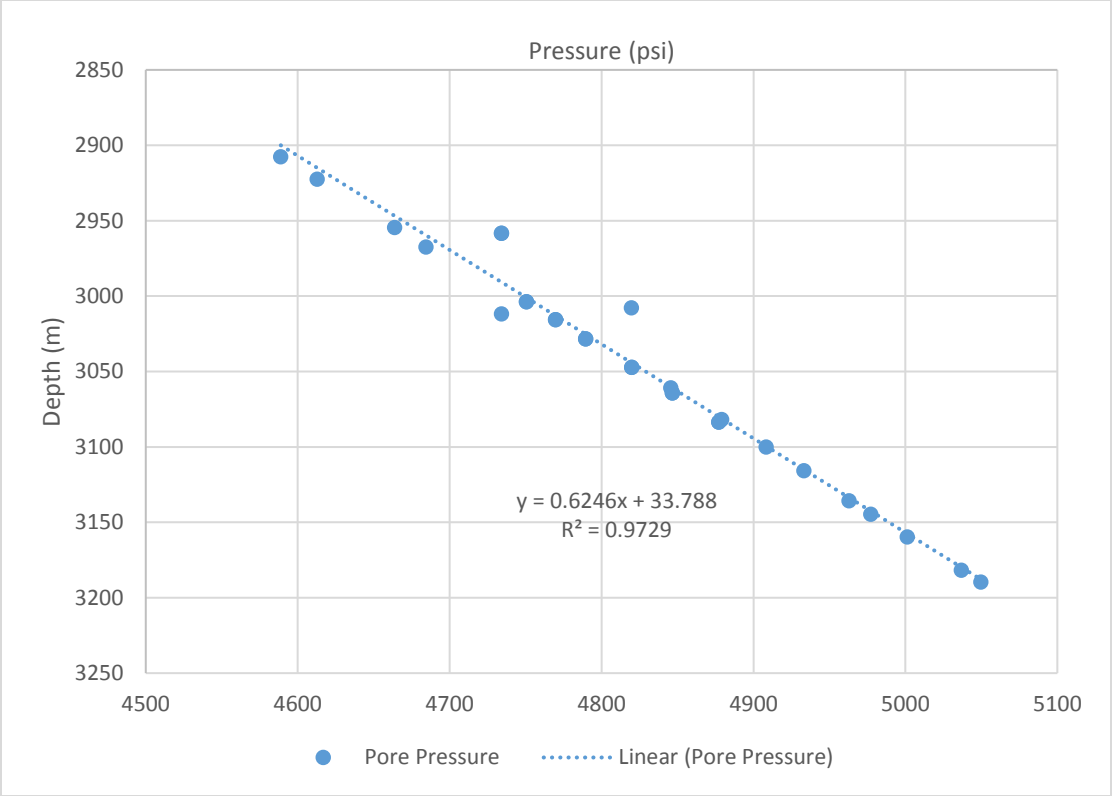

Figure 3.2. Pore pressure variation with respect to the depth.

3.4.2. Mechanical Rock Properties. The mechanical properties of the rock, such us elastic modulus (Young's modulus), Poisson's ratio, internal friction angle, and unconfined compressive strength (UCS), are derived by using an empirical equations. These equations are connected with five types of logs: compression and shear sonic (V_p & V_s), bulk density (ρ_b), neutron porosity, and gamma ray. Figure 3.3 illustrates the utilized logs for well H-10.

Additionally, the dynamic Young modulus is converted by using Equation 8. Equation 29 is used to derive the friction angle due to unavailability of the core sample. Figure 3.4 shows the calculated mechanical properties for Nahr Umr Formation.

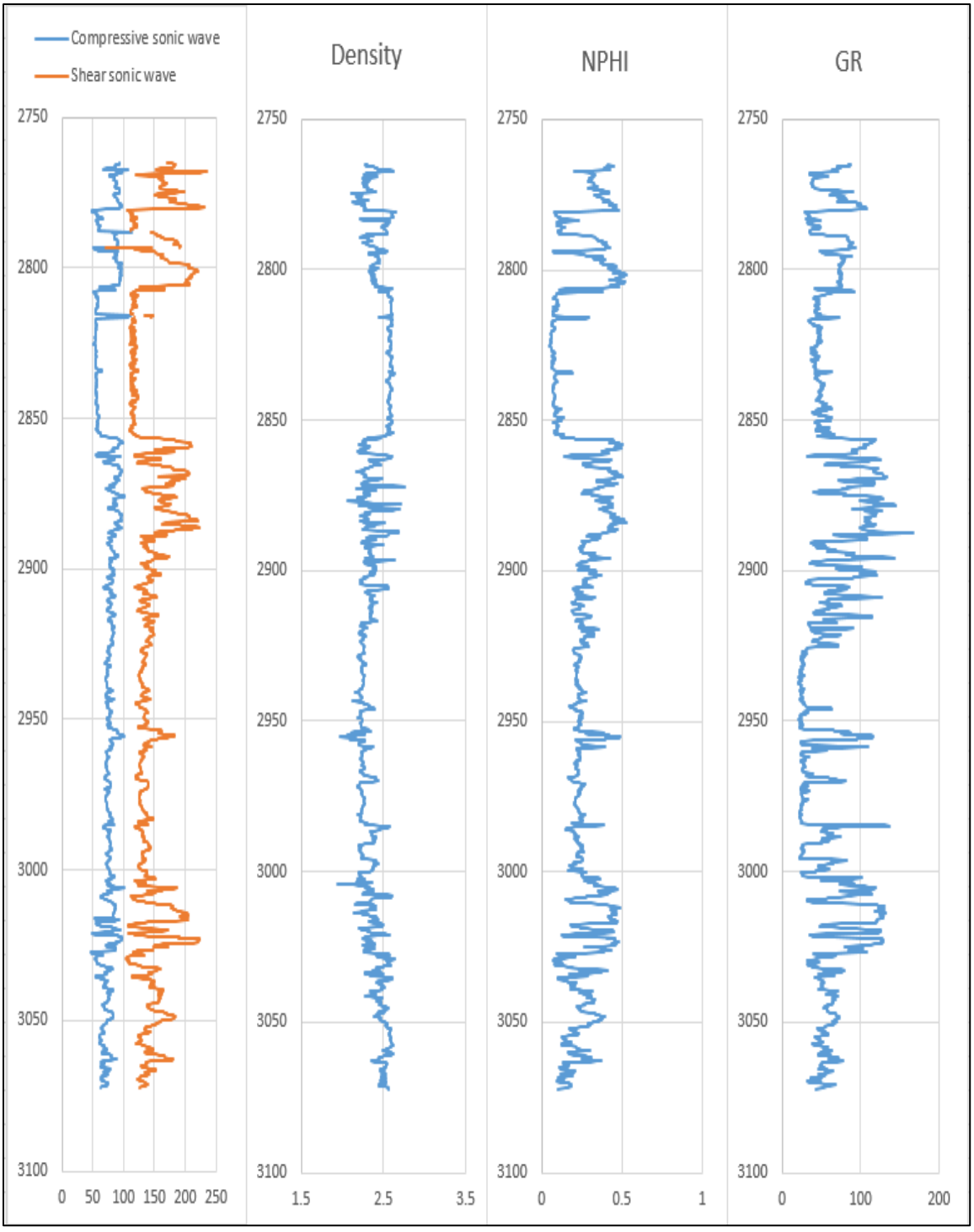

Figure 3.3. Well logs in well H-10.

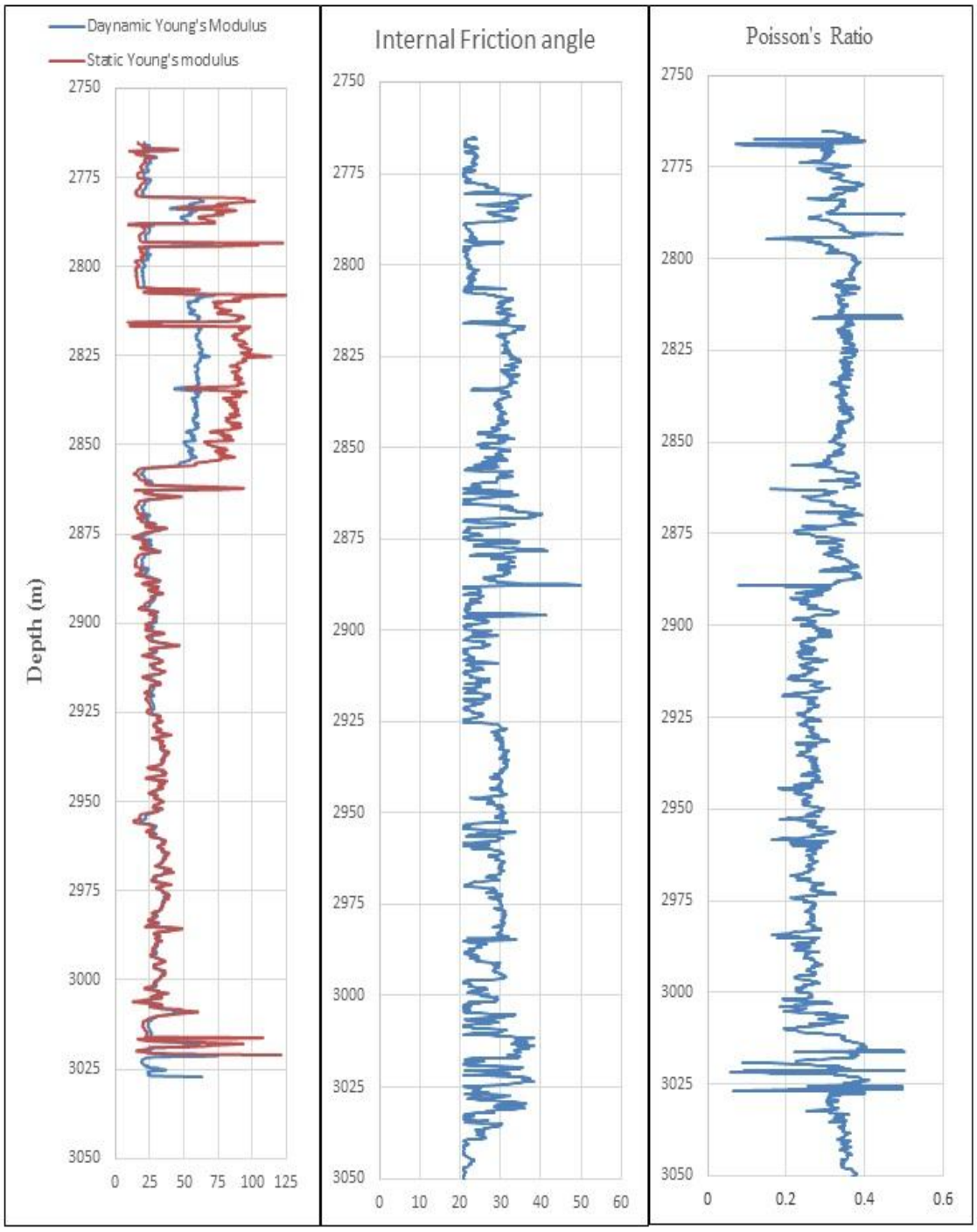

Figure 3.4. The mechanical properties in Nahr Umr Formation.

Due to the strong heterogeneity of Nahr Umr Formation, the UCS is estimated by using three empirical equations, such as Equation 31 for shale formation, Equation 32 for limestone, and Equation 33 for sandstone (Figure 3.5).

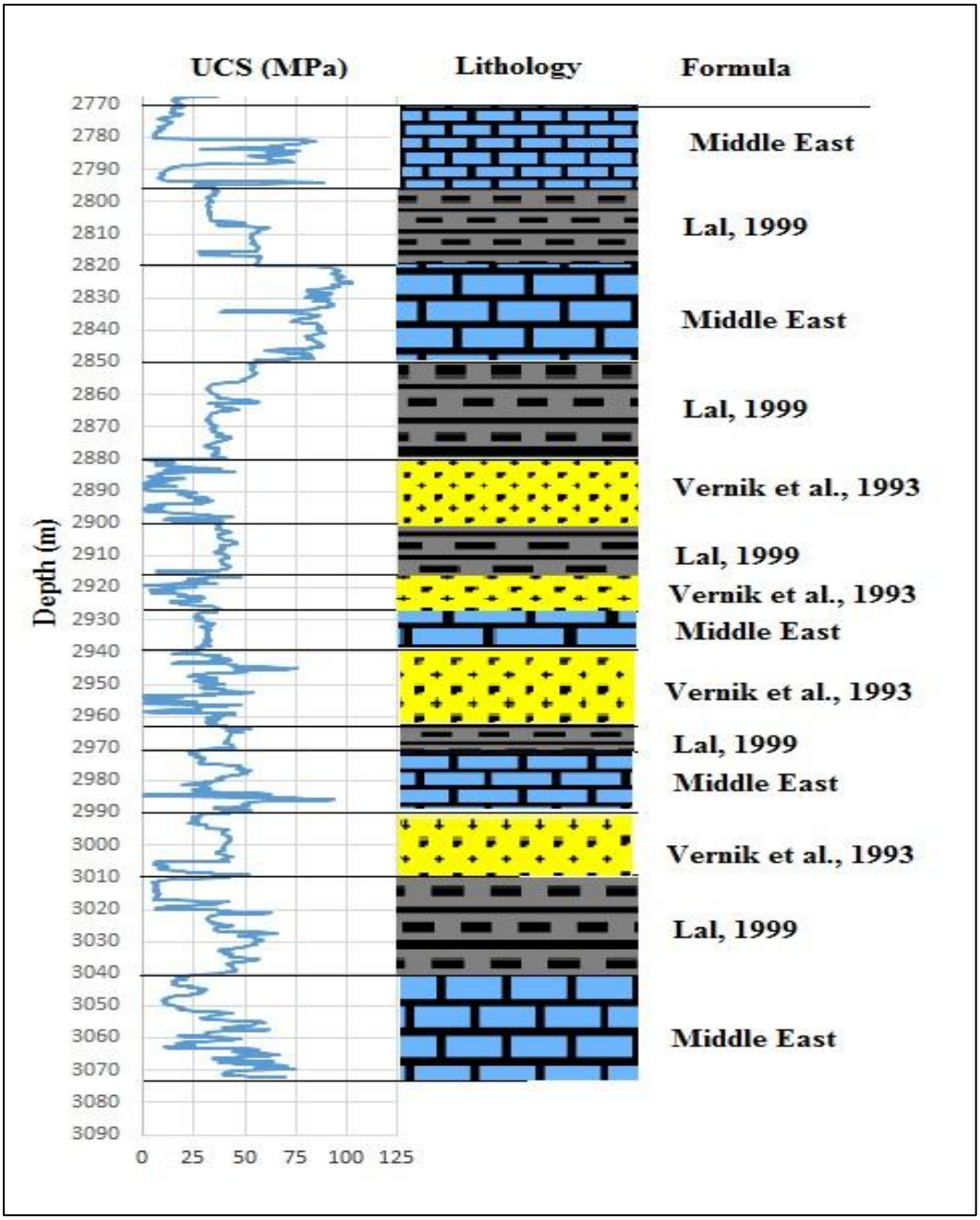

Figure 3.5. Confined compressive strength with respect to lithology heterogeneity.

3.4.3. In-Situ Stresses. The overburden stress (Sv) is estimated by integration of the rock densities Equation 12. Density logging tools were used in this analysis to obtain the bulk density (Bell, 1990a). The vertical stress of Nahr Umr Formation in well H-10 ranged from 58 Mpa to 72 Mpa. For the horizontal stresses, Hudson and Harrison (1997) summarized many direct and indirect approaches to estimation. In this study, the minimum horizontal stress (S_h) is estimated from the extended leak-off test (XLOT) (Zoback et al., 1985). The minimum horizontal stress is estimated to be 55.1 Mpa at a depth of 2970 m. In addition, empirical equations including Equations 14, 15, 16, and 19 are used to predict the minimum horizontal stress for the entire Nahr Umr section. The S_h value calculated from XLOT at depth 2970 is overlaid with the S_h values that are calculated from Holbrook et al. (1993) (Eq. 19). Thus, the Holbrook et al. (1993) equation is utilized to estimate the S_h for the entire Nahr Umr formation. Because there is no direct way to predict the value of maximum horizontal stress (S_H), Equation 20 is used to estimate the maximum horizontal stress. Figure 3.6 illustrates the in-situ stress profiles across the entire section. To evaluate the horizontal stresses, the stress polygon was used to estimate the allowed ranges of maximum and minimum horizontal stresses, Figure 3.7. The polygon results show that the normal faulting regime is dominate.

The minimum mud density is estimated by using a constitutive geomechanical model connected with two failure criteria (Mohr and Mogi). The input parameters for our geomechanical are summarized in Table 3.1. The recommended mud weight by using Mohr-Coulomb and Mogi-Coulomb are listed in Table 3.2.

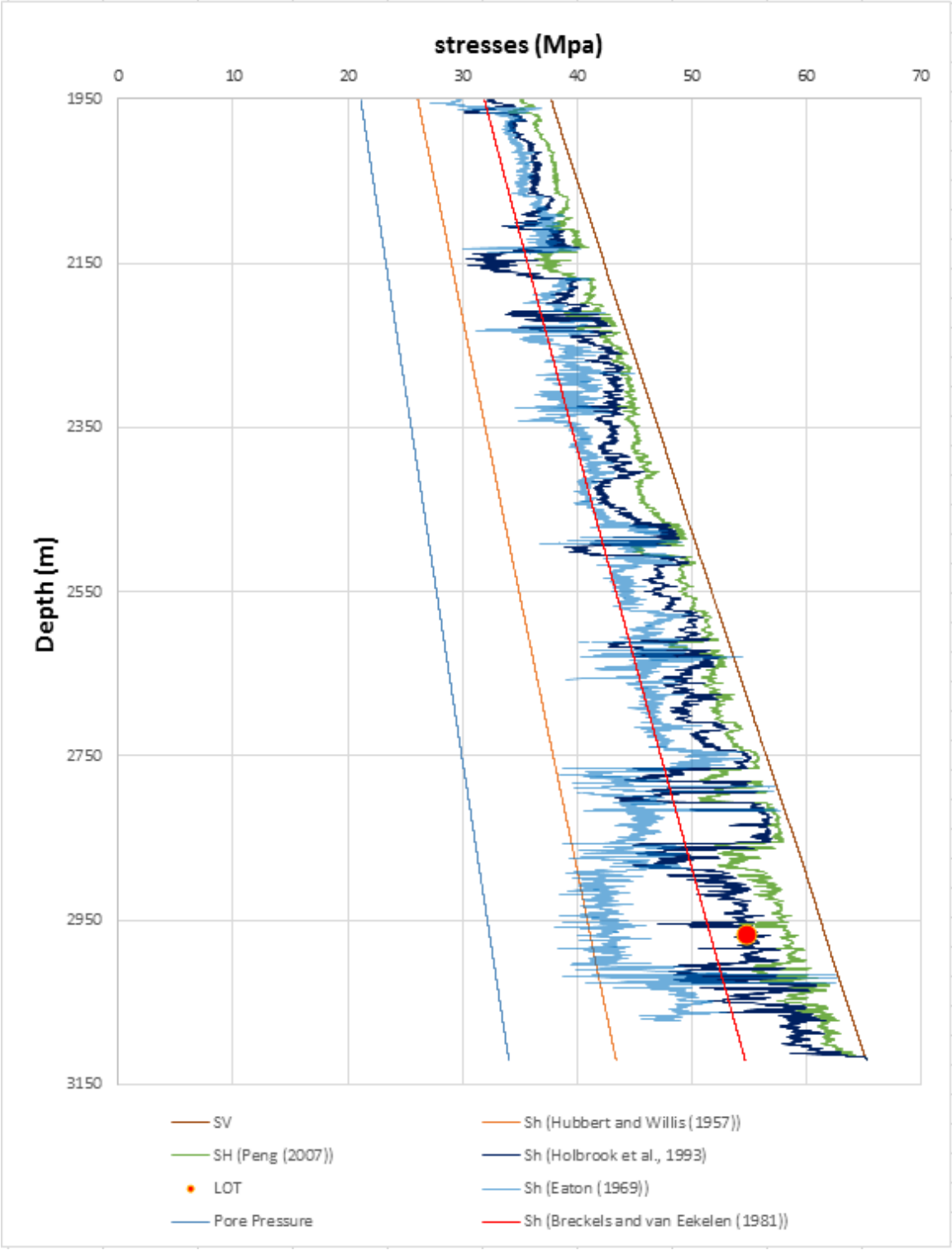

Figure 3.6. Stress profile through 12.25-in. hole section, case study 1.

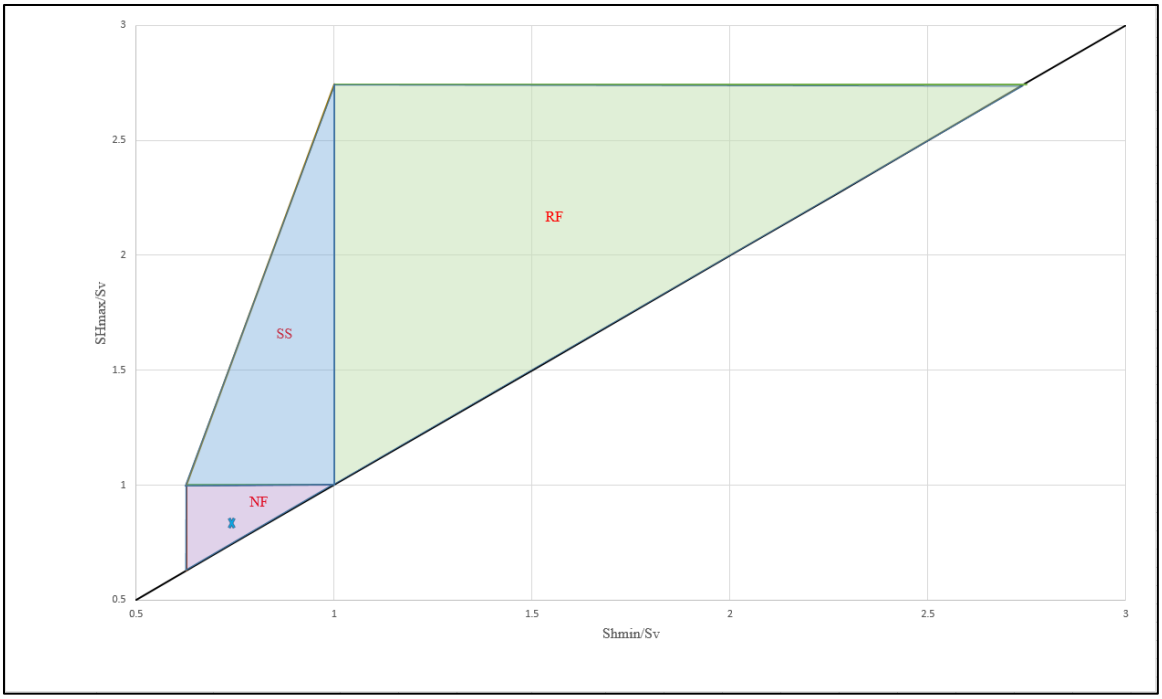

Figure 3.7. Nahr Umr Formation stress polygon.

Table 3.1. The input of the geomechanical model (In-situ stresses, Pore pressure, and mechanical properties), case study 1.

Parameters	Value	Unit	Source
Depth	2900	m	
Sv	60.15	Mpa	
SH	50	Mpa	Peng (2007)
Sh	45	Mpa	Holbrook et al. (1993)
Pp	31.6	Mpa	RFT
Poisson's ratio	0.23		
Young's modulus	23.5	Gpa	
UCS	20	Mpa	Lal (1999)
Friction angle	24.4		Plumb (1994)

Table 3.2. The output of the geomechanical models, case study 1.

	Used	Mohr-Coulomb	Mogi-Coulomb
MW (SG)	1.2	1.32	1.26

3.5. CASE STUDY 2

The H-2 well is part of H Field Development Plan; its objective is to provide water from Nahr Umr Formation and reinject the water by closed system in Cretaceous Mishrif Limestone in order to support the reservoir pressure decline. The well is located in the dome 2, which is the second largest dome in the H field. Instability problems such as caving and tight spots were observed during drilling the Nahr Umr Formation, the lithology description in the Well H-2 shows the same description as Well H-10. Case 1 procedure was followed to construct the stress profile, predict the rock strength properties, and optimum mud density for Well H-2. Figure 3.8 shows the in-situ stress and pore pressure. Rock strength properties and shale volume are displayed in Figure 3.9 and Figure 3.10. The input (in-situ stresses, rock strength properties, and pore pressure) and output parameters are listed in the Table 3.3 and Table 3.4, respectively.

3.6. CASE STUDY 3

The well H-8 is planned as a vertical hole with a total depth of 3610 m. Nahr Umr Formation was drilled with mud weight 1.2 SG. Several drag and tight spots, as well as shale caving (blocky and splintery with 2-4 cm in length), were observed while performing wiper trip in Nahr Umr Formation. The same empirical equations in case 1 were used to build the geomechanical model. Figure 3.11 shows the in-situ stress and pore pressure. The rock strength properties and shale volume are illustrated in Figure 3.12 and 3.13. Table 3.5 and 3.6 illustrated the input and output of the geomechanical model.

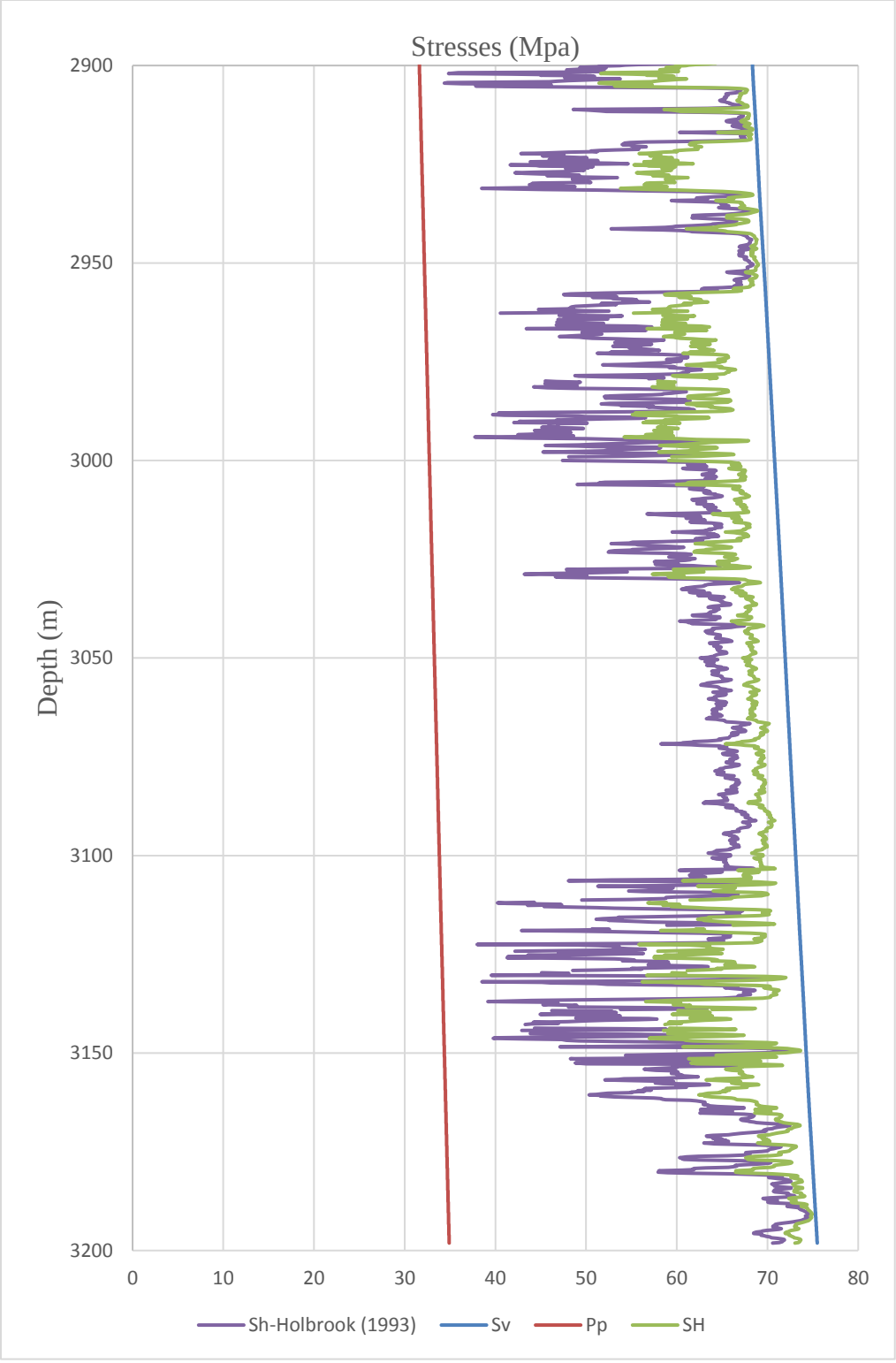

Figure 3.8. In-situ stresses and pore pressure profile though Nahr Umr Formation, case study 2.

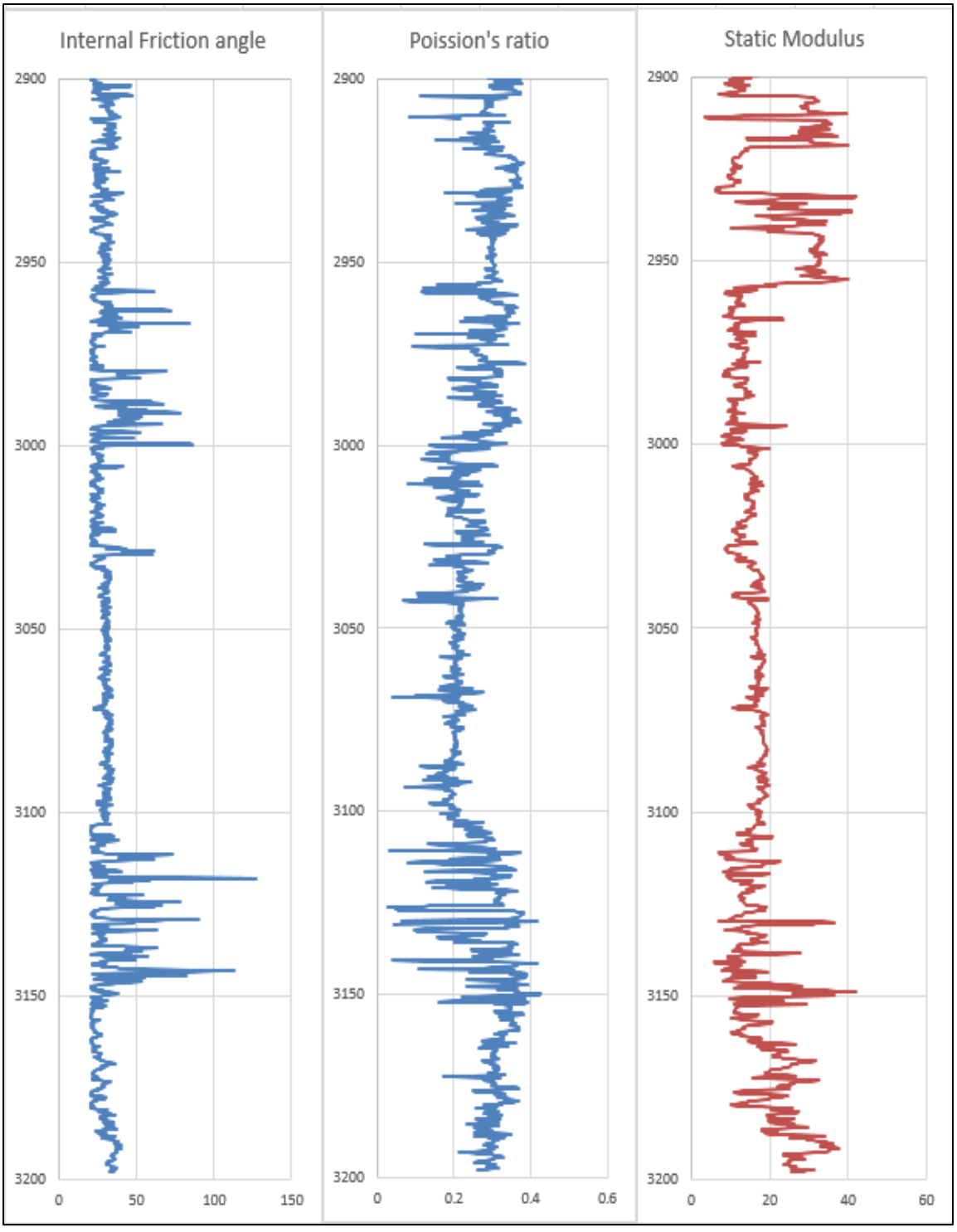

Figure 3.9. Rock strength parameters, case study 2.

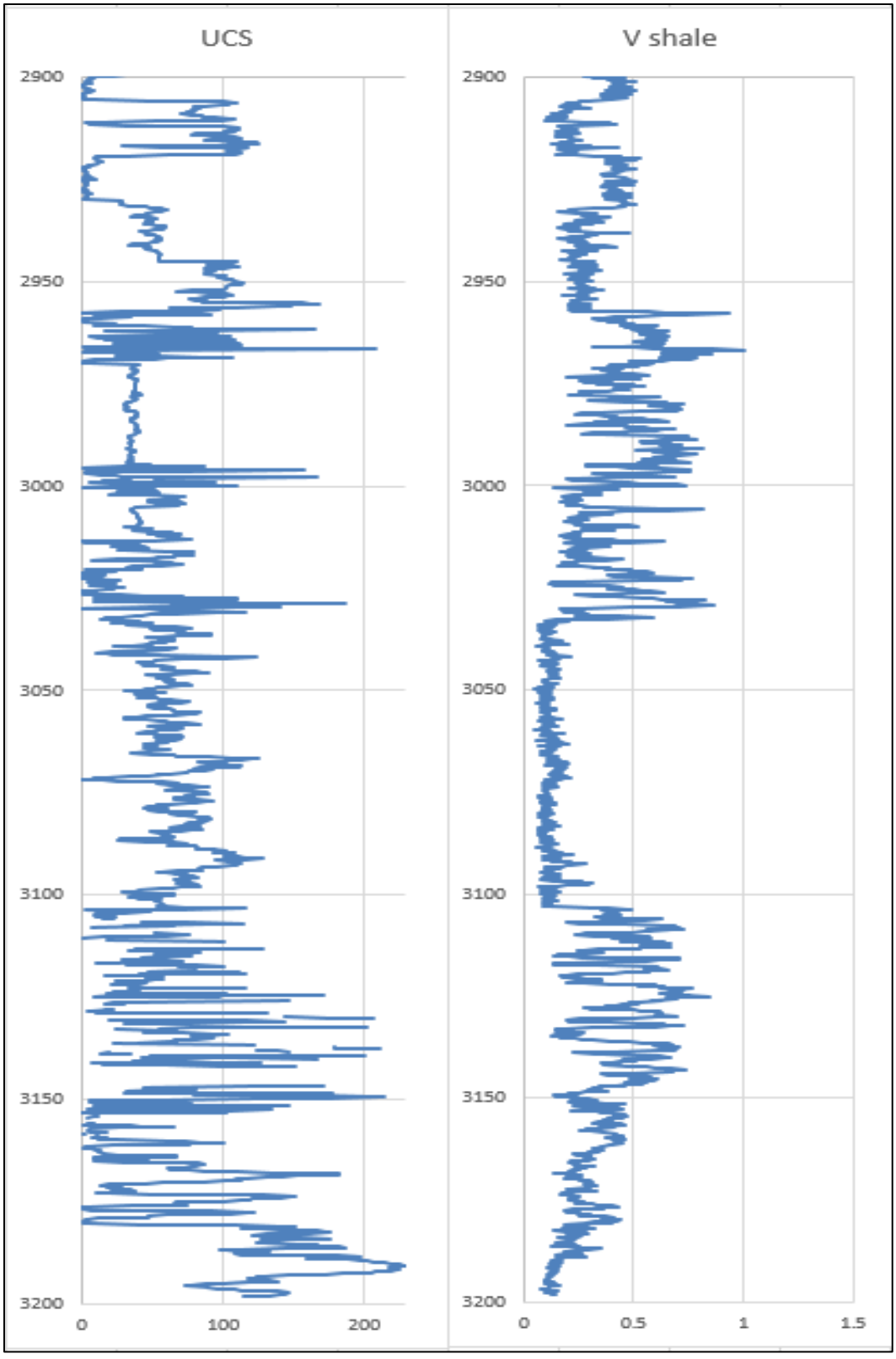

Figure 3.10. Shale volume and UCS, case study 2.

Table 3.3. The input of the geomechanical model, case study 2.

Parameters	Value	Unit	Source
Depth	2981	m	
Sv	70.35	Mpa	
SH	64	Mpa	Peng (2007)
Sh	47	Mpa	Holbrook et al. (1993)
Pp	32.5	Mpa	RFT
Poisson's ratio	0.28		
Static Young's modulus	12.5	Gpa	
UCS	31	Mpa	Lal (1999)
Friction angle	24.4		Plumb (1994)

Table 3.4. The output of the geomechanical model, case study 2.

	Used	Mohr-Coulomb	Mogi-Coulomb
MW (SG)	1.2	1.36	1.27

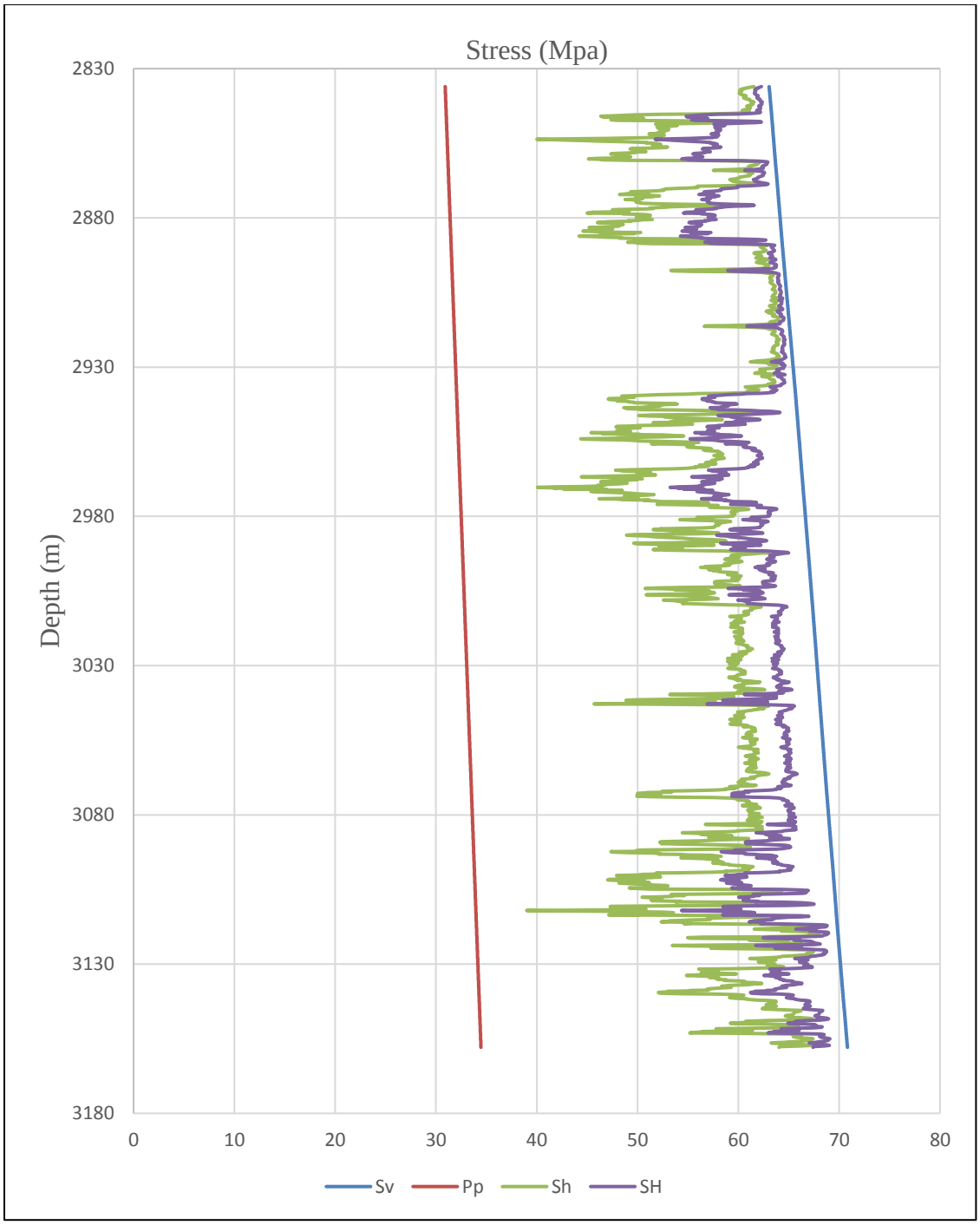

Figure 3.11. In-situ stresses and pore pressure profile though Nahr Umr Formation, case study 3.

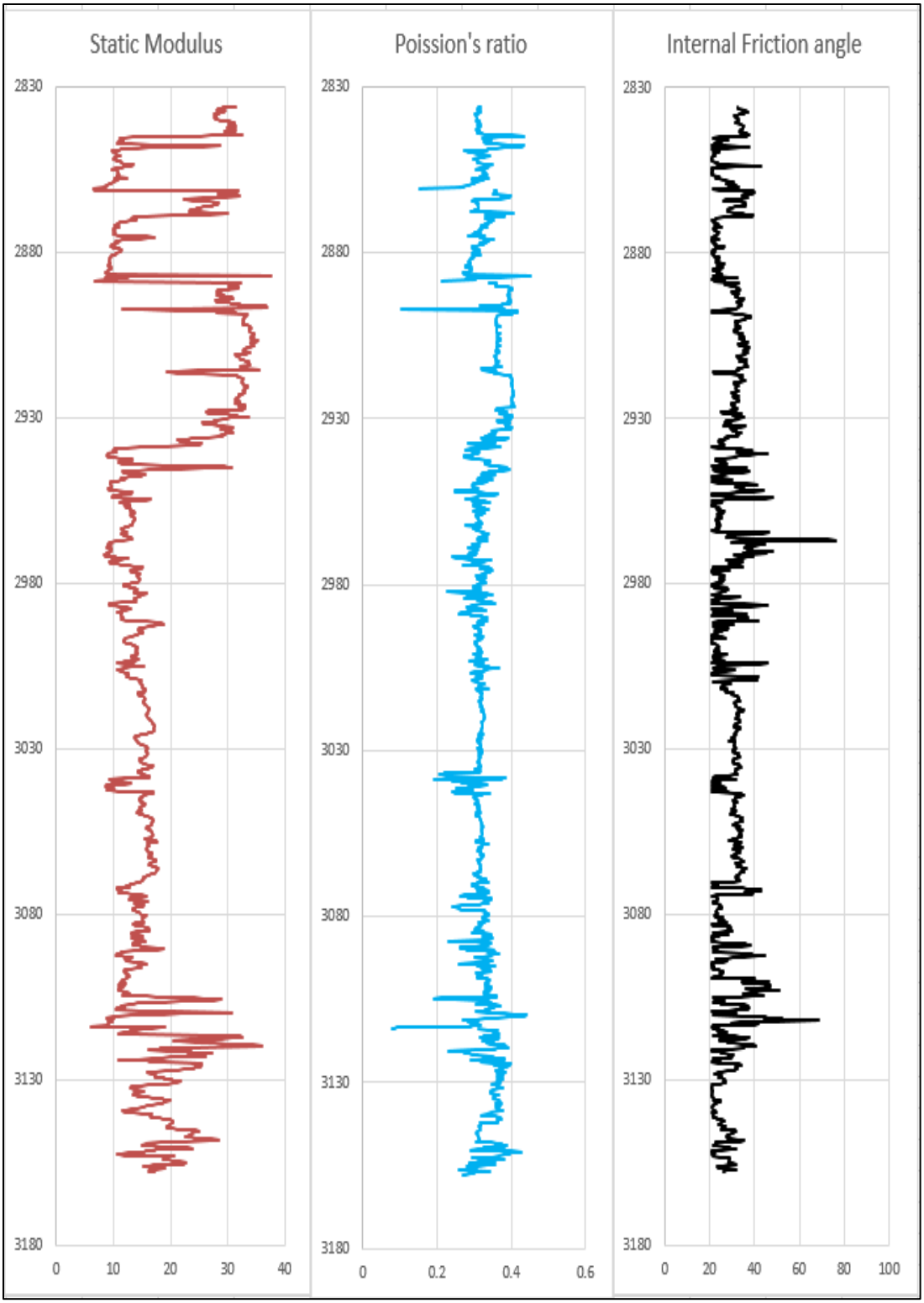

Figure 3.12. Rock strength parameters, case study 3.

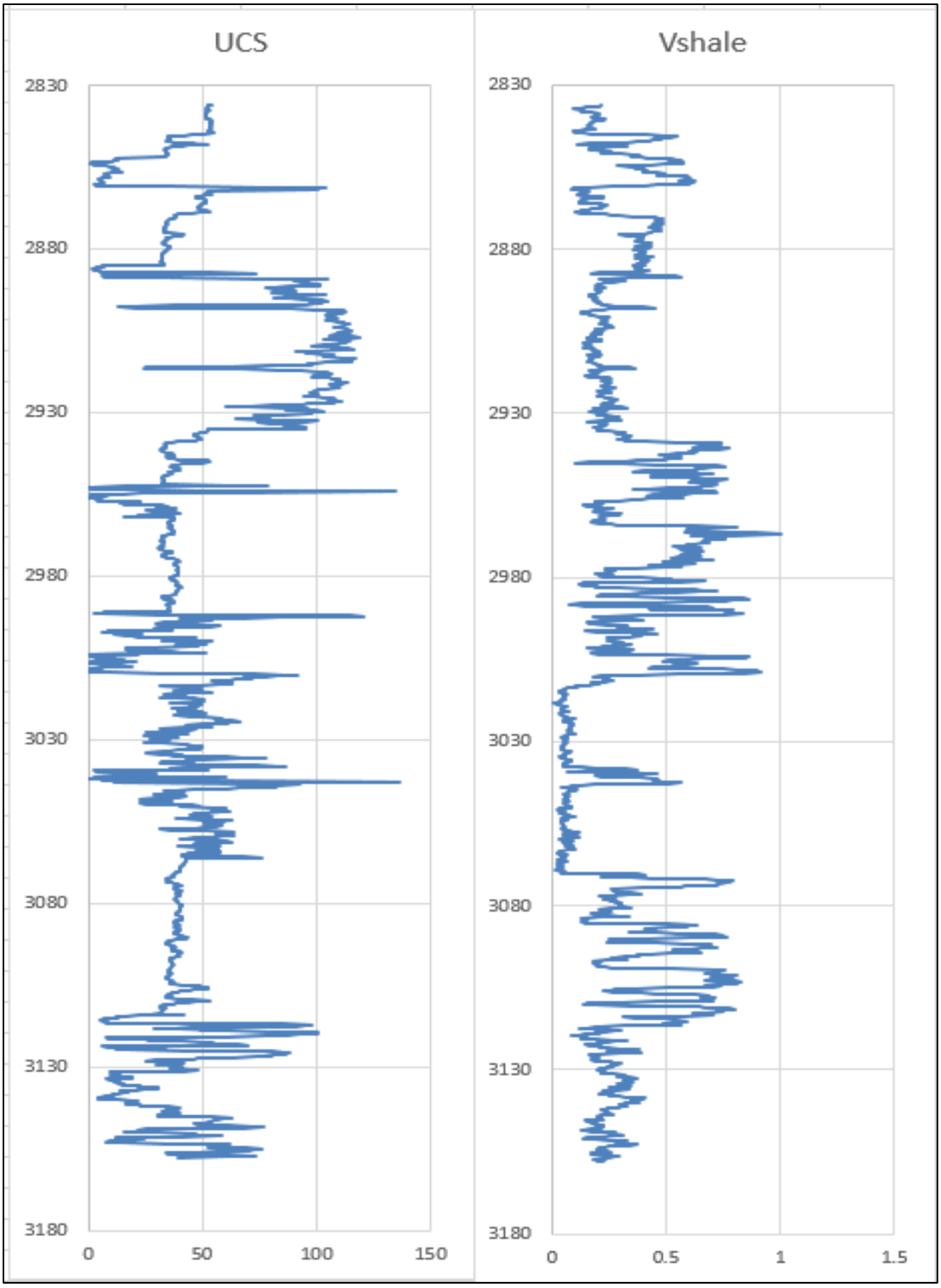

Figure 3.13. UCS and shale volume, case study 3.

Table 3.5. The input of the geomechanical model, case study 3.

Parameters	Value	Unit	Source
Depth	2880	m	
S_v	64.13	Mpa	
S_H	56.5	Mpa	Peng (2007)
S_h	50.6	Mpa	Holbrook et al. (1993)
P_p	31.39	Mpa	RFT
Poisson's ratio	0.29		
Static Young's modulus		Gpa	Lacy (1997)
UCS	32	Mpa	Lal (1999)
Friction angle	21		Plumb (1994)

Table 3.6. The output of the geomechanical model, case study 3.

	Used	Mohr-Coulomb	Mogi-Coulomb
MW (SG)	1.2	1.38	1.27

3.7. CASE STUDY 4

Several wellbore instability problems were faced while drilling Nahr Umr Formation in the Well H-6. These problems included tight spots, hard back reaming, and stuck pipe. The stuck pipe experience was encountered two times preceding by overpull reach to 40 tons. A geomechanical model was employed to predict optimum mud weight. In-situ stresses and pore pressure results are illustrated in Figure 3.14. Rock strength

properties and shale volume are depicted in Figure 3.15 and 3.16. The input and output of the geomechanical model are illustrated in Table 3.7 and 3.8, respectively.

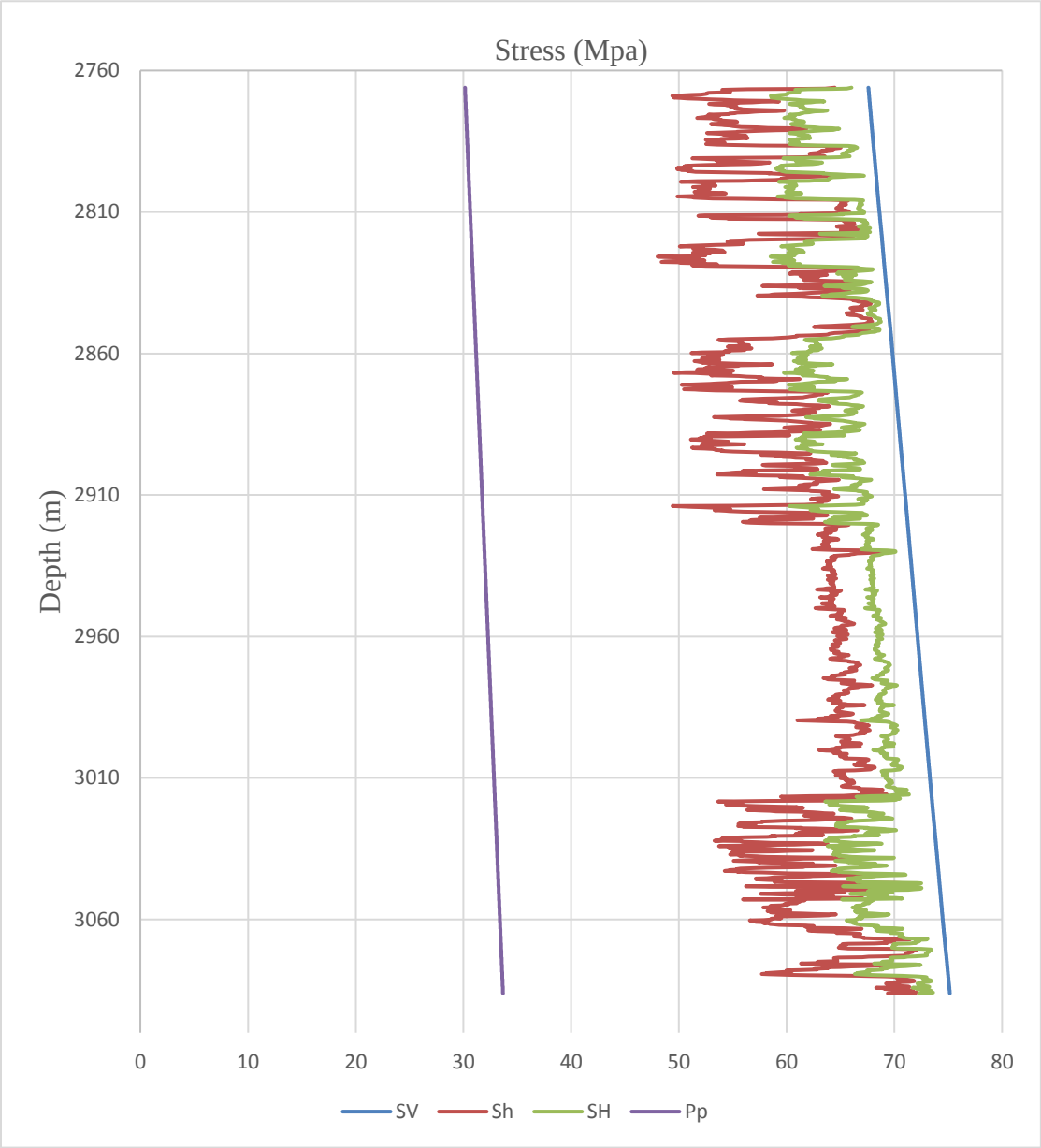

Figure 3.14. In-situ stresses and pore pressure profile though Nahr Umr Formation, case study 4.

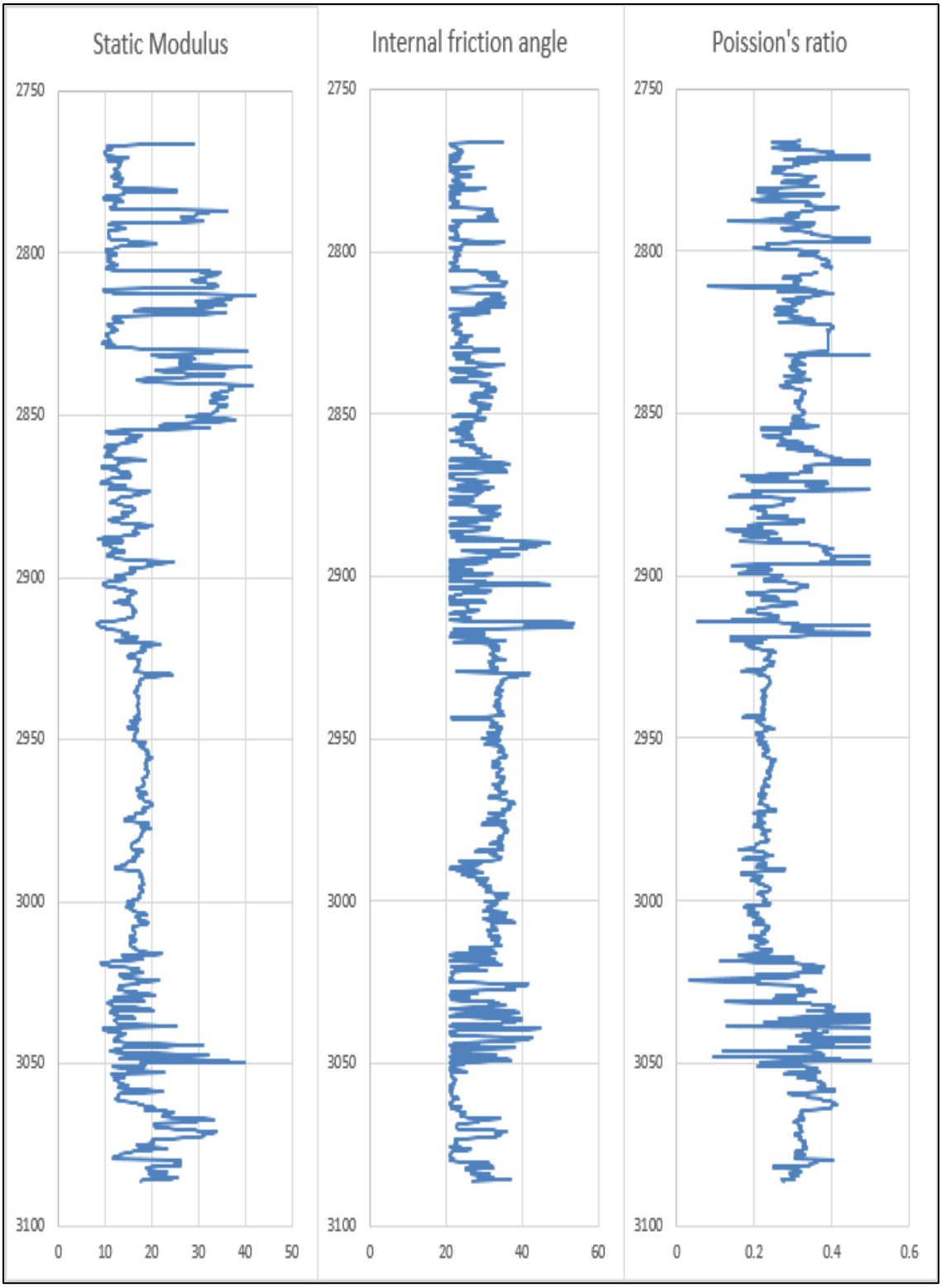

Figure 3.15. Rock strength parameters, case study 4.

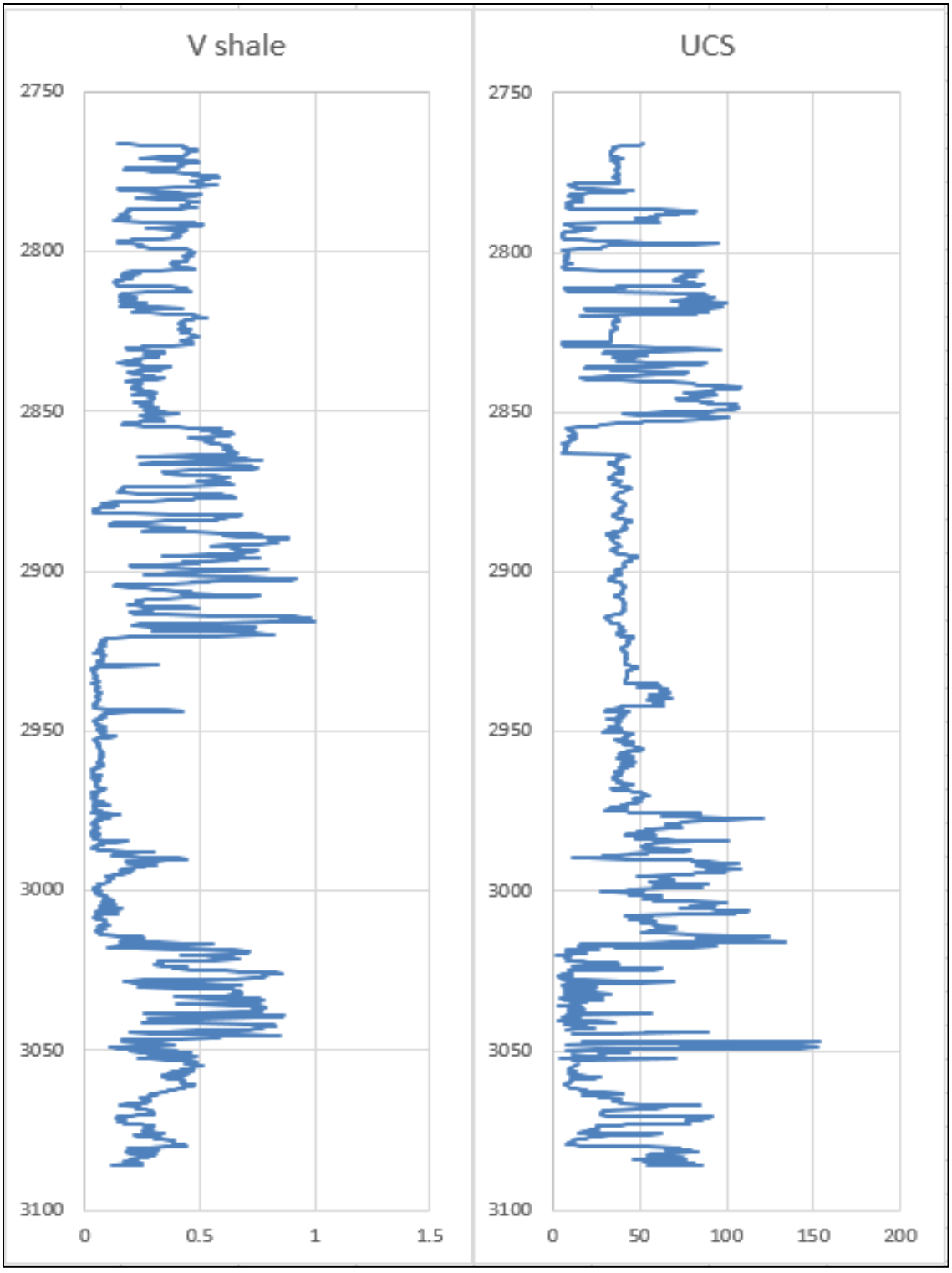

Figure 3.16. UCS and shale volume, case study 4.

Table 3.7. The input of the geomechanical model, case study 4.

Parameters	Value	Unit	Source
Depth	2890	m	
Sv	70.53	Mpa	
SH	63	Mpa	Peng (2007)
Sh	50	Mpa	Holbrook et al. (1993)
Pp	31.51	Mpa	RFT
Poisson's ratio	0.34		
Static Young's modulus	11.39	Gpa	
UCS	30	Mpa	Lal (1999)
Friction angle	38		Plumb (1994)

Table 3.8. The output of the geomechanical model, case study 4.

	Used	Mohr-Coulomb	Mogi-Coulomb
MW (SG)	1.2	1.38	1.28

Input and output parameters of the geomechanical model for five cases are summarized in Table 3.9.

Table 3.9. Input and output of the geomechanical model for five cases.

	Case 1	Case 2	Case 3	Case 4	Case 5
Depth	2900	2981	2880	2890	2920
Sv	60.15	70.35	64.13	70.53	65.21
SH	50	64	56.5	63	55.6
Sh	45	47	50.6	50	49
SH Orientation	45°-50°	45°-50°	45°-50°	45°-50°	45°-50°
Pp	31.6	32.5	31.39	31.51	31.9
UCS	20	31	32	30	29
Friction angle	24.4	24.4	21	38	32
Poisson's ratio	0.23	0.28	0.29	0.34	0.29
Young's Modulus	23.5	12.5	10.4	11.39	12.3
Used MW	1.2	1.2	1.2	1.2	1.25
Related-problems	Breakout and stuck pipe	Tight spots	Breakout and tight spots	Stuck pipe and tight spots	No problems
Mogi-Coulomb	1.26	1.27	1.27	1.28	1.27
Mohr-Coulomb	1.32	1.36	1.38	1.38	1.38

3.8. SENSITIVITY ANALYSIS

A sensitivity analysis for geomechanical input parameters was conducted by using a tornado chart, Figure 3.17, to predict the effect of these parameters on the mud pressure design. The analysis reveals that the two horizontal stresses have a major effect on the mud pressure, with maximum horizontal stress having the greatest effect. In addition, the vertical stress and the internal friction angle showed a minor impact. Pore pressure and unconfined compressive strength came in the middle with intermediate effect.

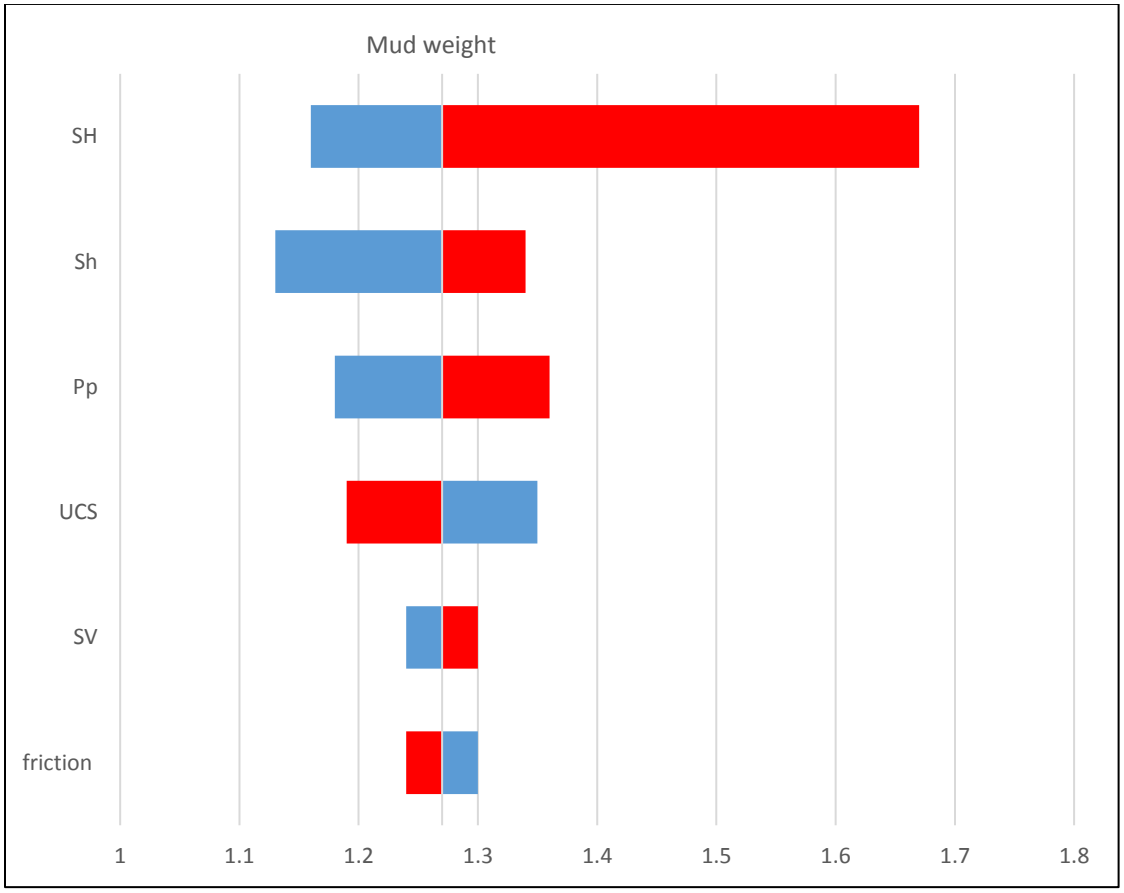

Figure 3.17. Contribution of the input parameters on the geomechanical model output.

4. DISCUSSION AND CONCLUSION

4.1. DISCUSSION

The 1D geomechanical modeling approach presented here is used to provide a more accurate representation of stable mud window by applying a geomechanical analysis incorporated with two failure criteria: Mohr-Coulomb and Mogi-Coulomb. This model is applied to five vertical wells to analyze the mechanical stability in the Nahr Umr Formation H oil field. These wells were selected based on the instability issue (stuck pipe, caving, and tight spots) and the location of the wells according to field domes. Well log data, final well reports, daily mud reports, mud logging reports, and field tests were investigated to predict the causes and majority of wellbore instability. Based on the data investigation the in-situ stresses and pore pressure profile, and rock strength was built. The results show that the vertical stresses in the five wells ranges between 56.9 and 75.4 Mpa, and there is linear increasing between vertical stress and depth. I addition, the pore pressure shows the same behavior of vertical stress (a linear relationship with depth). Figure 3.6 shows the horizontal stresses magnitudes based on different correlations. The correlations of Hubberts and Willis (1957) and Breckels and Van Eeckelen (1981) show a linear propagation with depth, while those from Holbrook et al. (1993) and Eaton (1969) show high fluctuations in the horizontal stresses through the interval. This fluctuation was caused by the variety of porosity and Poisson's ratio. Holbrook et al. (1993) showed the best representative of S_h in the field due to overlay with the LOT value. The Peng (2007) equation was used to predict the value of maximum horizontal stress. The results in Figure 3.6 show high fluctuation due to the variety in the value of S_h through the interval. Due to the high heterogeneity in the Nahr Umr Formation, three empirical equations were used to predict the value of UCS:

sandstone, limestone, and shale correlations. As can be seen in Figure 3.5, the UCS trend shows a high value in the limestone interval, but tends to decrease when the shale volume increases (Figure 3.15). On the other hand, the rock strength parameters in Figure 3.4 show the same behavior of UCS (Young's modulus and the internal friction angle tend to increase in the limestone intervals). As can be seen in the output tables, the four wells were drilled with 1.2 SG mud weight; the results show that the used mud weight is less than that required to sustain the borehole wall. The Mohr-Coulomb failure criterion predicts the optimum mud weight to be between 1.32 and 1.38 SG, and Mogi-Coulomb predicts the optimum mud weight between 1.26 and 1.28. Vernik and Zoback (1992) pointed out that Mohr-Coulomb failure criterion did not provide realistic results. Recently, Rahimi and Nygaard (2015) alluded that the Mohr-Coulomb predicition showed overestimated value, while the Mogi-Coulomb prediction was more reliable. In addition, comparing the mud weight of 1.25 SG that has been used in the successful wells (well number five) and the geomechanical model outputs shows that Mogi-Coulomb produces a reasonable prediction of 1.26-1.28 SG and it is in close agreement with field observation.

4.2. CONCLUSION

This research presents a case study in the Nahr Umr Formation of oil fields in southern Iraq. Through this study, the following conclusions can be made:

1- This investigation reveals that the majority of the drilling events that caused most of the NPT while drilling in Nahr Umr Formation are mostly caused by high stresses and low rock strength and inappropriate drilling practice with respect to the heterogeneity of Nahr Umr Formation.

2- A geomechanical model was developed using two failure criteria. The analysis of the output of the geomechanical model shows that the Mogi-Coulomb criterion gives more appropriate results than the Mohr-Coulomb criterion (Mogi-Coulomb was in close agreement with field observation). This was related to the fact of Mohr-Coulomb criterion underestimates the rock strength by disregarding the effect of intermediate principle stress. In contrast, the Mogi-Coulomb criterion becomes more realistic by considering the effect of intermediate stress on rock strength.

3- Wellbore breakout observation with resistivity image log (star image log) show that the surrounding area of the wellbore fails due to the strong control of the orientation and magnitude of the in-situ stresses.

4- Based on the horizontal stresses orientations, the recommended safe drilling in the inclination or directional wells will be along the minimum horizontal stress direction which is between 135-140°.

5- The rock strength tests and field tests are useful in the calibration of the mechanical earth modeling.

6- Several wellbore collapses, stuck pipe, and shale caving (wellbore failure) were observed in the Nahr Umr Formation. This wellbore failure was due to using insufficient mud weight and not considering an appropriate geomechanical analysis.

7- Normal fault regime is the dominate regime in the H-field ($S_v > S_H > S_h$).

BIBLIOGRAPHY

Aadnoy, B. S. (2003). "Introduction to special issue on wellbore stability." Journal of Petroleum Science and Engineering 38: 79-82.

Aadnoy, B. S., 1989b. Stresses around horizontal boreholes drilled in sedimentary rocks. J Petrol Sci Eng, 2[4], 349-360.

Aadnoy, B. S., Ong, S., 2003. Introduction to special issue on Borehole Stability. J Petrol SciEng, 38[3-4], 79-82.

Aadnoy, B., & Chenevert, M. (1987). Stability of Highly Inclined Boreholes (includes associated papers 18596 and 18736). SPE Drilling Engineering, 2(04), 364-374. doi:10.2118/16052.

Addis, M. A., Last, N. C., & Yassir, N. A. (1996, March 1). Estimation of Horizontal Stresses at Depth in Faulted Regions and Their Relationship to Pore Pressure Variations. Society of Petroleum Engineers. doi:10.2118/28140-PA.

Adnoy, B., and Looyeh, R. (2010). Drilling operations and well design.

Al-Ajmi, A. M., & Zimmerman, R. W. (2005). Relation between the Mogi and the Coulomb failure criteria. International Journal of Rock Mechanics and Mining Sciences, 42(3), 431-439. doi:10.1016/j.ijrmms.2004.11.004.

Al-Husseini, M.I. 2000. Origin of the Arabian Plate structures; Amar collision and Najd Rift. GeoArabia, v. 5, no. 4, p. 527-542.

Alsubaih, A. A., & Nygaard, R. (2016, June 26). Shale Instability of Deviated Wellbores in Southern Iraqi Fields. American Rock Mechanics Association.

Anderson, E. M., 1951. The dynamics of faulting. Oliver & Boyd, Edinburgh. Geomechanics: Bridging the Gap from Geophysics to Engineering in Unconventional Reservoirs. (n.d.). Retrieved March 06, 2017, from http://csegrecorder.com/articles/view/geomechanics-bridging-the-gap-from-geophysics-to-engineering.

Andrews, L, J.. Abu Lihie, O., Makhlous, I., Abu Saad, L., Tanni, Y., Al-Bashaish, M. and Al-Hiayri, A., 1991. Palaeozoic Stratigraphy in the subsurface of Jordan. Publication of the Natural Resource Authority, Jordan, 65P.

Anthony, J. L. and Crook, J. Y., 2002. Development of an orthotropic 3D elastoplastic material model for shale. In: Proc SPE/ISRM Rock Mech Conf, Irving, Texas, October 20-23. SPE 78238.

Aqrawi, A. A, Horbuury, A. D., Goff, J. C., and Sadooni, F. N. (2010). Petroleum Geology of Iraq. Scientific Press Ltd.

Avasthi J.M., Goodman H.E., Jansson R.P., March 2000. Acquisition. Calibration, and Use of the In-Situ Stress Data for Oil and Gas Well Construction and Production. SPE-60320.

Awal, M. R., Khan, M. S., Mohiuddin, M. A., and Abdulraheem, A., 2001. A new approachto borehole trajectory optimisation for increased hole stability. In: Proc SPE Middle East Oil Show, Bahrain, 17-20 March. SPE 68092.

Barton, C.A., Moos, D., Peska, P., and Zoback, M. 1997, Utilizing Wellbore Image Data to Determine the Complete Stress Tensor: Application to Permeability Anisotropy and Wellbore Stability: The Log Analyst, p. 21-33.

Bell, J. (2003). Practical methods for estimating in situ stresses for borehole stability applications in sedimentary basins. Journal of Petroleum Science and Engineering, 38(3-4), 111-119.

Bell, J.S., (1990) a, investigation stress regimes in sedimentary basins using information from oil industry wireline logs and drilling records, in Hurst, A., ed., Geological society of London, special publication 48, p. 305-32.

Bell, J.S., Gough, D.I., 1979. Northeast-southwest compressive stress in Alberta evidence from oil wells. Earth Planet. Sci. Lett. 45 (2), 475–482.

Bellen, R.C., Dunnington, H.V., Wetzel, R. and Morton, D. (1959) Lexique Stratigraphique International Asie, Iraq. Vol. 3C, 10a, 333 p.

Biot, M.A., 1941. General theory of three-dimensional consolidation. J. Appl. Phys. 12(1):155-164.

Bradley, W. B., 1979. Mathematical concept-stress cloud can predict borehole failure. Oil Gas J, 77[8], 92-102.

Breckels, I. M. and Van Eekelen, H. A. M. (1981). "Relationship between horizontal stress and depth in sedimentary basins: Paper SPE10336, 56th Annual Fall Technical Conference." Society of Petroleum Engineers of AIME, San Antonio, Texas, October 5–7, 1981.

Breckels, I. M., & van Eekelen, H. a. M. (1982). Relationship Between Horizontal Stress and Depth in Sedimentary Basins. Journal of Petroleum Technology, 34(September), 2191–2199. http://doi.org/10.2118/10336-PA.

Brew, G., R. Litak, M. Barazangi and T. Sawaf 1999. Tectonic evolution of Northeast Syria: regional implications and hydrocarbon prospects. GeoArabia, v. 4, no. 3, p. 289–318.

Bourgoyne, A.T., Chenevert, M.E., Millheim, K.K. and Young, F.S., 1986. Applied Drilling Engineering, 2. SPE, Richardson, TX.

Chang, C., Zoback, M. D., & Khaksar, A. (2006). Empirical relations between rock strength and physical properties in sedimentary rocks. Journal of Petroleum Science and Engineering, 51(3-4), 223-237. doi:10.1016/j.petrol.2006.01.003.

Chen, X., Tan, C. P., Haberfield, C. M., 2002. A comprehensive, practical approach for wellbore instability management. SPE Drilling Comp, 17[4], 224-236.

Detournay,E. and Cheng,A. H.-D. (1988). Poroelastic response of a borehole in a nonhydrostatic stress field, Int. J. Rock Mech.,25,171–82.

Ding, D. (2011). Coupled simulation of near-wellbore and reservoir models. Journal of Petroleum Science and Engineering, 76(1-2), 21-36. doi:10.1016/j.petrol.2010.12.004.

Douban A.F. and F. Al-Medhadi 1999. Sequence chronostratigraphy and petroleum system of the Cretaceous megasequences, Kuwait. American Association of Petroleum Geologists International Conference.

Eaton, B. A. (1969). Fracture Gradient Prediction and Its Application in Oilfield Operations. Journal of Petroleum Technology, 21(10), 1353–1360. http://doi.org/10.2118/2163-PA.

Eaton, B. A., 1975, The equation for geopressure prediction from well logs: 50th Annual Technical Conference, Paper 5544, 11.

Engelder T. 1993. Stress Regimes in the Lithosphere. Princeton University Press.

Ewy, R. (1999). Wellbore-Stability Predictions by Use of a Modified Lade Criterion. SPE Drilling & Completion, 14(02), 85-91. doi:10.2118/56862-pa.

Fairhurst, C., 1965b. On the determination of the state of stress in rock masses. In: Procannual AIME Meeting, Chicago, Feb.14-18. SPE1062.

Fjaer E., Holt, R., Horsrud, P., Raaen, A.,Risnes, R. (2008). Petroleum related rock mechanics. 2nd ed. Amsterdam, Netherlands. Elsevier.

French, F. R. and McLean, M. R., 1992. Development drilling problems in high-pressure reservoirs. In: Proc SPE Int Meeting Petrol Eng, Beijing, 24-27 March. SPE 22385.

Furst, M., 1970. Stratigraphie and Werdegang der Oestlichen Zagrosketten Iran, Erlanger. Geol. Abhandlungen, 80, Erlangen.

Gentzis, T., Deisman, N., & Chalaturnyk, R. J. (2009). A method to predict geomechanical properties and model well stability in horizontal boreholes. International Journal of Coal Geology, 78(2), 149-160. doi:10.1016/j.coal.2008.11.001.

Gnirk, P. P., 1972. The mechanical behaviour of uncased wellbores situated in elastic/plastic media under hydrostatic stress. Soc Petrol Eng J, February, 49-59. SPE 3224.

Haimson, B. and Fairhurst, C. (1967). "Initiation and Extension of Hydraulic Fractures in Rocks."Soc. Petr. Eng. Jour., Sept.: 310–318.

Han, G., Timms, A., Henson, J., & Aziz, I. A. (2009). Wellbore Stability Study: Lessons and Learnings From a Tectonically Active Field. Asia Pacific Oil and Gas Conference & Exhibition. doi:10.2118/123473-ms

Herget, G., 1988. Stresses in Rock, Balkema, Rotterdam.

Holbrook, P.W., Maggiori, D. A. et al. (1993). Real-time pore pressure and fracture gradient evaluation in all sedimentary lithologies, SPE 26791.Offshore European Conference, Aberdeen, Scotland, Society of Petroleum Engineers.

Howard, J. A., & Glover, S. B. (1994, January 1). Tracking Stuck Pipe Probability While Drilling. Society of Petroleum Engineers. doi:10.2118/27528-MS.

Howard, J.A., Glover, S.B. 1994. Tracking Stuck Pipe Probability While Drilling. Presented at SPE/IADC Drilling Conference, Dallas, Texas, 15 – 18 February. SPE-27528-MS. http://dx.doi.org/10.2118/27528-MS.

Hubbert, M. K. and Willis, D. G. (1957). "Mechanics of hydraulic fracturing." Petr. Trans. AIME,210, 153–163.

Hubbert, M. K., & Willis, D. G. (1957, January 1). Mechanics Of Hydraulic Fracturing. Society of Petroleum Engineers.

Hudson, J.A., Harrison, J.P., 1997. Engineering rock mechanics, An Introduction to the Principles, 1st ed. Pergamon.

Iraq. (n.d.). Retrieved April 20, 2017, from http://www.opec.org/opecweb/en/about_us/164.htm.

Jaeger, J.C., Cook, N.G., Zimmerman, R., 2009. Fundamentals of Rock Mechanics.John Wiley & Sons.

Jassim, S. Z., & Goff, J. C. (2006). Geology of Iraq. Prague and Moravian Museum Zelny trh 6, Brno, Czech Republic.

Jørgensen T., Fejerskov M. 1998. Leak-Off Tests: How to extract important in-situ stress information from a test originally designed for another purpose. SPE/ISRM Eurock '98, Trondheim, Norway, 8–10 July.

Lade, P.V.: "Failure Criterion for Frictional Materials," Mechanics of Engineering Materials , C.S. Desai and R.H. Galager (eds.), John W iley & Sons, New York City (1984) 385.

Lal, M., 1999. Shale stability: drilling fluid interaction and shale strength. SPE Latin American and Caribbean Petroleum Engineering Conference held in Caracas, Venezuela.

Lama RD, Vutukuri VS, 1978. Handbook on mechanical properties of rocks. Clausthal,Germany: Trans. Tech. Publications;

Manshad, A. K., Jalalifar, H., & Aslannejad, M. (2014). Analysis of vertical, horizontal and deviated wellbores stability by analytical and numerical methods. Journal of Petroleum Exploration and Production Technology, 4(4), 359-369. doi:10.1007/s13202-014-0100-7.

Mansourizadeh, M., Jamshidian, M., Bazargan, P., & Mohammadzadeh, O. (2016). Wellbore stability analysis and breakout pressure prediction in vertical and deviated boreholes using failure criteria – A case study. Journal of Petroleum Science and Engineering, 145, 482-492. doi:10.1016/j.petrol.2016.06.024

Meng, F., Fuh, G.F., 2013. Wellbore Stability Evaluation Guideline for Reducing Non-Productive Time, Presented in International Petroleum Technology Conference.

Mitchell, R. F., Goodman, M. A., and Wood, E. T., 1987. Borehole stresses: plasticity and the drilled hole effect. In: Proc IADC/SPE Drilling Conf, New Orleans, March 15-18. SPE16053.

Mogi, K. (1971). Fracture and flow of rocks under high triaxial compression. Journal of Geophysical Research, 76(5), 1255-1269. doi:10.1029/jb076i005p01255.

Pariseau, W.G., 2006. Design analysis in rock mechanics, 1st ed. Taylor & Francis.

Paslay, P. R. and Cheatham, J. B., 1963. Rock stresses induced by flow of fluids into boreholes. Soc Pet Eng J, 3[1], 85-94. SPE 482.

Peng S, Ling B, Liu D (2002a) Application seismic CT detection technique into roof coal caving comprehensive mechanical longwall mining. Chinese Rock Mech Eng 21(12):1786-1790 (in Chinese).

Peng S, Wang X, Xiao J, Wang L, Du M (2001) Seismic detection of rockmass damage and failure zone in tunnel. J China Univ Min Tech 30(1):23-26 (in Chinese).

Peng, S. and Zhang, J. (2007). Engineering Geology for underground rocks. Springer-Verlag Berlin Heidelberg.

Plumb, R. (1994). Influence of composition and texture on the failure properties of clastic rocks. Rock Mechanics in Petroleum Engineering. doi:10.2118/28022-ms.

Plumb, R.A. and S.H. Hickman (1985): Stress-induced borehole enlargement: a comparison between the four-arm dipmeter and the borehole televiewer in the Auburn geothermal well. - J. Geophys. Res., 90, 5513-5521.

Rabia, H., 1985. Oilwell Drilling Engineering. Principles & Practice, Graham & Trotman.

Rahimi, R. (n.d.). The effect of using different rock failure criteria in wellbore stability analysis (Unpublished master's thesis).

Risnes, R. and Bratli, R. K., 1981. Sand stresses around a wellbore. In: Proc Middle East Oil Tech Conf Soc Petrol Eng, Manama, Bahrain, March 9-12. SPE 9650.

Ronald Steiger, P. R., Leung, K. peter (1992). "Quantitative Determination of the Mechanical Properies of Shales." SPE 7.

Ruzhnikov, A. (2013). Stability of production section in south Iraq. Oil and Gas Business, (6), 58-80. doi:10.17122/ogbus-2013-6-58-80.

Standifird WB, Paine K, Matthews MD (2004) Improving drilling success requires better technology and models. World oil 225(10):51-56

Terzaghi, K., Peck, R.B., Mesri, G., 1996. Soil Mechanics in Engineering Practice (3rd Edition). John 811 Wiley & Sons.

Tutuncu, A. N., Geilikman, M., Couzens, B., & Duyvenboode, F. V. (2006). Integrated wellbore-quality and risk-assessment study guides successful drilling in Amazon jungle. Geophysics, 71(6). doi:10.1190/1.2356257.

TWISS, R. J. & MOORES, E. M. 2006. Structural Geology, New York, W. H. Freeman and Company. ULA TAMBAR SUBSURFACE TEAM 2013. Ula Hub Development. BP.

Veatch, R. W., & Moschovidis, Z. A. (1986, January 1). An Overview of Recent Advances in Hydraulic Fracturing Technology. Society of Petroleum Engineers. doi:10.2118/14085-MS.

Vernik, L., & Zoback, M. D. (1992). Estimation of maximum horizontal principal stress magnitude from stress-induced well bore breakouts in the Cajon Pass Scientific Research borehole. Journal of Geophysical Research, 97(B4), 5109. doi:10.1029/91jb01673.

Vernik, L., Bruno, M., Bovberg, C., 1993. Empirical relations between compressive strength and porosity of siliciclastic rocks. Int. J. Rock Mech. Min. Sci. Geomech. Abstr. 30, 677–680.

Waragai, T., Yamamoto, K., & Tokuda, N. (2006). Eliminating Additional Drilling Expense Due to Well Stability Problem in Laminated/Fractured Nahr Umr Shale Formation. Abu Dhabi International Petroleum Exhibition and Conference. doi:10.2118/101383-ms.

Westergaard, H. M., 1940. Plastic state of stress around a deep well. J Boston Soc Civil Eng,27, 1-5.

Wikel, K. (2011, May 01). Geomechanics: Bridging the Gap from Geophysics to Engineering in Unconventional Reservoirs. Retrieved April 14, 2017, from http://csegrecorder.com/articles/view/geomechanics-bridging-the-gap-from-geophysics-to-engineering

Yamamoto K. 2003. Implementation of the extended leak-off test in deep wells in Japan. In: Sugawra K, editor. Proceedings of the 3rd international symposium on rock stress. Rotterdam: A.A. Balkema. p. 225–9.

Yamamoto, K., Shioya, Y., Matsunaga, T., Kikuchi, S., & Tantawi, I. (2002). A Mechanical Model Of Shale Instability Problems Offshore Abu Dhabi. Abu Dhabi International Petroleum Exhibition and Conference. doi:10.2118/78494-ms.

Zhang, J., Bai, M., & Roegiers, J. (2003). Dual-porosity poroelastic analyses of wellbore stability. International Journal of Rock Mechanics and Mining Sciences,40(4), 473-483. doi:10.1016/s1365-1609(03)00019-4

Zhang, J., Lang, J., & Standifird, W. (2009). Stress, porosity, and failure-dependent compressional and shear velocity ratio and its application to wellbore stability. Journal of Petroleum Science and Engineering, 69(3-4), 193-202. doi:10.1016/j.petrol.2009.08.012

Zoback, M. D. (2007). Reservoir Geomechanics. doi:10.1017/cbo9780511586477

Zoback, M. D. and Healy, J. H. (1984). "Friction, faulting, and "in situ" stresses." Annales Geophysicae,2, 689–698.

Zoback, M. D., Mastin, L., & Barton, C. (1986, August 31). In-situ Stress Measurements In Deep Boreholes Using Hydraulic Fracturing, Wellbore Breakouts, And Stonely Wave Polarization. International Society for Rock Mechanics.

Zoback, M. D., Moos, D., Mastin, L., & Anderson, R. N. (1985). Well bore breakouts and in situ stress. Journal of Geophysical Research, 90(B7), 5523. doi:10.1029/jb090ib07p05523.

Zoback, M., Barton, C., Brudy, M., Castillo, D., Finkbeiner, T., Grollimund, B., . . . Wiprut, D. (2003). Determination of stress orientation and magnitude in deep wells. International Journal of Rock Mechanics and Mining Sciences, 40(7-8), 1049-1076. doi:10.1016/j.ijrmms.2003.07.001.

VITA

Haider Qasim Mohammed was born in Baghdad, Iraq in 1988. He received his bachelor's degree in petroleum engineering from Baghdad University, Baghdad, Iraq in 2010. He started working in South Oil Company, a Petroleum Iraqi Company, in the Drilling and Completion Department in 2010. He spent most of his work as Drilling Supervisor. Haider was selected by Higher Committee for Education Development in Iraq (HCED), which belongs to the Prime Ministry of Iraq, to study for a master's degree in petroleum engineering. He arrived in Missouri in January 2015 and started his study in the Intensive English Program (IEP) in Rolla, Missouri which lasted for two semesters. In Fall 2015 semester, he began his academic study at Missouri University of Science and Technology under supervision of Dr. Ralph E. Flori. He received a Master of Science degree in Petroleum Engineering from Missouri University of Science and Technology in July 2017.